

EFFECTS OF LOW IMPACT DEVELOPMENT DESIGN ON REDOX DYNAMICS
IN THE VADOSE ZONE AND URBAN GROUNDWATER

AS
36
2015
GEOL
•D36

A Thesis submitted to the faculty of
San Francisco State University
In partial fulfillment of
The requirements for
The Degree

Master of Science

In

Geosciences

by

Mays Nakhleh Danfoura

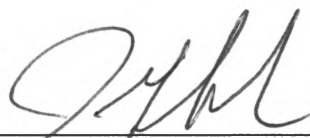
San Francisco, California

January 2015

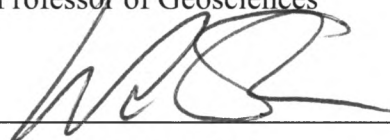
Copyright by
Mays Nakhleh Danfoura
2015

CERTIFICATION OF APPROVAL

I certify that I have read Effects of Low Impact Development Design on Redox Dynamic in the Vadose Zone and Urban Groundwater by Mays N. Danfoura, and that in my opinion this work meets the criteria for approving a thesis submitted in partial fulfillment of the requirement for the degree Master of Science in Geosciences at San Francisco State University.



Jason Gurdak, Ph.D.
Professor of Geosciences



Leonard Sklar, Ph.D.
Professor of Geosciences



Bruce Manning, Ph.D.
Professor of Chemistry

EFFECTS OF LOW IMPACT DEVELOPMENT DESIGN ON REDOX DYNAMICS IN THE VADOSE ZONE AND URBAN GROUNDWATER

Mays Nakhleh Danfoura

San Francisco, California

2015

Low impact development (LID) best management practices (BMPs) collect, infiltrate, treat urban runoff, and increase recharge to aquifers. Therefore, understanding the redox conditions beneath LID BMPs is essential from a groundwater management perspective. In this study, the influence of design features of a LID BMP infiltration trench on the dynamics of dissolved oxygen (DO) in infiltrating stormwater was investigated. The magnitude and duration of fluctuations in DO concentrations in the LID infiltration trench were found to be influenced by hydraulic conditions in the gravel with an inverse relation between the duration of % saturation in the gravel and DO concentrations. DO reached anoxic levels within hours to days, which strongly indicates that microbial respiration activities are a limiting factor of DO in the gravel. However, temperature of stormwater was not found to exhibit a major influence on redox dynamics in the infiltration trench. The estimated O_2 reduction rate for the infiltration trench was found to be 0.003 mg/L minute, which is 2 to 5 orders of magnitude higher than the O_2 reduction rates for groundwater aquifers estimated in previous studies. Higher rates of O_2 reduction in the infiltration trench are a function of the more oxic flow system and of the higher source of organic matter from stormwater input. The estimated O_2 reduction rate in this study strongly indicates denitrification processes are promoted within the gravel. The observed low oxic and anoxic conditions triggered by infiltration of stormwater in the LID infiltration trench are expected to carry on downward through the gravel and probably into the sub-soils beneath and eventually into groundwater. Altering the design of LID BMPs to manipulate redox processes can be an important tool to minimize groundwater contamination.

I certify that the Abstract is a correct representation of the content of this thesis.


Chair, Thesis Committee

12-17-2014
Date

ACKNOWLEDGEMENTS

I would like to express my appreciation and gratitude to my advisor, Jason Gurdak, for his support throughout the development process of my master's thesis. I would also like to acknowledge my committee members, Leonard Sklar and Bruce Manning, for their support, useful comments and remarks.

Partial funding of this research was provided by the Dawdy Hydrology Research Grant. I would like to thank Doris and David Dawdy for their generous contributions. I would also like to thank my family and friends for their assistance, especially my husband, Fred Danfoura, who has supported and encouraged me throughout this process.

TABLE OF CONTENTS

LIST OF TABLES	VIII
LIST OF FIGURES	IIIX
1.0 Introduction.....	1
1.1. Background and Problem Statement.....	1
1.2. Low Impact Development.....	3
1.3. Reduction/Oxidation (Redox).....	4
1.4. Objectives and Hypothesis.....	6
2.0 Methods.....	8
2.1. Study Area	8
2.2. Saturation of Gravel.....	9
2.3. Vadose Zone Data Collection	10
2.4. Precipitation	11
2.5. Runoff.....	13
2.6. Rate of O ₂ Reduction	14
2.7. LID Oxygen Demand Rate	14
3.0 Results	16
3.1. Precipitation	16
3.2. Water Levels	17
3.3. Saturation of Gravel.....	18
3.4. Water Temperature	20
3.5. Specific Conductance.....	22
3.6. Dissolved Oxygen.....	23
3.7. Rate of O ₂ Reduction	26
3.8. LID Oxygen Demand Rate (LIDOD)	27

4.0 Discussion.....	27
5.1. Dynamics of Water Level, Temperature and Conductivity in LID Trench under Stormwater Runoff Influence	27
5.2. DO Dynamics in Response to Saturation of Gravel	30
5.3. DO Dynamics in Response to Duration of Saturation in Gravel	32
5.4. DO Dynamics in Response to Change in Water Temperature	35
5.5. Rate of O ₂ Reduction and Denitrification.....	36
5.6. Design of LID BMP.....	39
5.0 Conclusion	41
6.0 References.....	45
7.0 Figures and Tables.....	51

LIST OF TABLES

Table 1. Soil textural and hydraulic properties for cores collected at the infiltration trench.....	75
Table 2. Precipitation Frequency Estimates for Downtown station, San Francisco.	75
Table 3. Zero-order rates of O ₂ reduction for wells 1 and 3, for 6 rain event during the period of field observation of DO (February – June, 2014).	76
Table 4. LIDOD _T and LIDOD ₂₀ rates in mg/m ³ hour for wells 1 and 3, for 3 rain event during the period of field observation of DO (February – June, 2014).	76
Table 5. Corresponding durations of saturation and DO concentrations for rain events that occurred between February and April 2014 for well 1.....	77
Table 6. Corresponding durations of saturation and DO concentrations for rain events that occurred between February and April 2014 for well 3.....	78

LIST OF FIGURES

Figure 1. Map showing the location of the San Francisco State University (SFSU) low impact development (LID) research network and the Westside Basin aquifer, which is part of the California Coastal Basin aquifers. The aquifer location data are modified from the California Department of Water Resources and the U.S. Geological Survey. Modified from Newcomer et al., 2014.	51
Figure 2. Photographs of the infiltration trench at the San Francisco State University (SFSU) low impact development (LID) research network. Modified from Newcomer et al., 2014.....	51
Figure 3. Cross-section of the infiltration trench and the three piezometers with pressure transducers.	52
Figure 4. Schematic depiction (not to scale) of the instrumentation and core locations along the longitudinal cross-section A–A' (inset) of the infiltration trench site at the San Francisco State University (SFSU) low impact development (LID) research network. Modified from Newcomer et al., 2014.....	52
Figure 5. Schematic depiction (not to scale) of the miniDot oxygen loggers and pressure transducers instrumentation and core locations along the infiltration trench site at the San Francisco State University (SFSU) low impact development (LID) research network near (a) Well 1 and (b) Well 3.	53
Figure 6. Depth-duration-frequency curve for the San Francisco, Downtown station (NOAA NWS, 2014).	54
Figure 7. Annual exceedance probability for the San Francisco, Downtown station (NOAA NWS 2014).	54
Figure 8. Daily precipitation data from the San Francisco, Downtown station (Station ID: 047772) for the entire data collection period at the LID BMP (July 2012–June 2014) (NOAA NCDC, 2014).	55
Figure 9. Well#1 (a) hourly timeseries of precipitation. (b) water level in piezometers (c) temperature and (d) Specific Conductance for the period of field observation (July 2012 – June 2014).....	56
Figure 10. Well#2 (a) hourly timeseries of precipitation. (b) water level in piezometers. (c) temperature and (d) specific conductance for the period of field observation (July 2012 – June 2014).....	57

Figure 11. Well#3 (a) hourly timeseries of precipitation. (b) water level in piezometers (c) temperature and (d) specific conductance for the period of field observation (July 2012 – June 2014).....	58
Figure 12. Timeseries of Precipitation (black) and Water levels (blue) in (a) Well 1 (b) Well 2 and (c) Well 3 during rainfall events from November 19, 2012 – December 9, 2012.....	59
Figure 13. Timeseries of precipitation and % saturation in gravel for all three wells during the rainy season of 2013.	60
Figure 14. Timeseries of precipitation and % saturation in gravel for all three wells during the rainy season of 2014.	61
Figure 15. Timeseries for rain events and water temperature occurred on October 31- November 01, 2012, December 20-28, 2012, and March 30 – April 02, 2013 for wells 1, 2, and 3.....	62
Figure 16. Water levels (blue) and specific conductance (red) for (a) Well 1 (b) Well 2 and (c) Well 3 from November 20 - December 11, 2012.	63
Figure 17. DO concentrations measured continuously by the miniDot loggers in LID trench for the period of field observation February – June 2014 for (a) Well 1 and (b) Well 3.....	64
Figure 18. Timesereis of precipitation, water level, temperature, specific conductance, and DO concentrtration in the LID trench during two rainfall events ((a) February 15 to March 2, 2014, and (b) March 5 to March 8, 2014) of increasing precipitation depth and duration for Well 1.....	65
Figure 19. timesereis of precipitation, water level, temperature, specific conductance, and DO concentration in the LID trench during two rainfall events ((a) February 15 to March 2, 2014, and (b) March 5 to March 8, 2014) of increasing precipitation depth and duration for Well 3.	66
Figure 20. Concentrations of DO in the infiltration trench (during 6 rain events) as a function of elapsed time between beginning of rain event and lowest DO values for that particular rain event, for well 1. Linear regression statistics for the fit of zero-order reaction rate R (mg/L min) are shown for each rain event.	67
Figure 21. Concentrations of DO in the infiltration trench (during 6 rain events) as a function of elapsed time between beginning of rain event and lowest DO values for that particular rain event, for well 3. Linear regression statistics for the fit of zero-order reaction rate R (mg/L min) are shown for each rain event.	68

Figure 22. DO depletion curve for a) well 1 and b) well 3 for 3 rain events during the period of field observation (February – June, 2014). The slope of the linear fit for each oxygen-depletion curve [mg/l minute] is used to calculate an average slope of oxygen-depletion curve for the entire infiltration trench.	69
Figure 23. Timeseries of hourly % saturation in gravel (red), DO concentrations (blue), and hourly precipitation (gray) for a) well 1 and b) well 3. % saturation data for the period between March 29 and April 05, 2014 is missing.	70
Figure 24. Scatter plot of average and minimum DO vs. duration of saturation for 6 rain events during the period of field observation of DO (February – June 2014) for a) well 1 and b) well 3. General trend shows a negative correlation between the duration of saturation and average and minimum concentrations of DO.....	71
Figure 25. Timeseries of precipitation, DO concentrations, and water temperature for rain events during February – April, 2014, for a) well 1 and b) well3. Numbers above and below temperature series (red) refer to water temperatures under that particular rain event.	72
Figure 26. Oneway analysis of DO value for 6 rain events during the period of field observation of DO (February – June, 2014), for well 1.....	73
Figure 27. Oneway analysis of DO value for 6 rain events during the period of field observation of DO (February – June, 2014), for well 3.....	74

1.0 Introduction

1.1. Background and Problem Statement

Surface water and groundwater resources are interrelated through physical (streams, lakes, reservoirs, wetlands, and estuaries) and chemical interactions. Degradation of surface-water quality may result in a corresponding degradation of groundwater quality (Winter 1999). Urbanization has an adverse effect on the supply and quality of water resources (Pitt et al. 1995, Paul and Meyer 2001), largely because of increases in impervious surfaces, compaction of soils, and modifications to vegetation (Elliott and Trowsdale 2007; Maniquiz et al 2010). This results in reduction of infiltration and thus increases the volume of surface runoff (Fletcher et al 2013). Impervious surfaces like pavement, rooftops, and parking lots increase storm runoff volume and contaminant loads in stormwater. Stormwater runoff from the impervious surfaces can be contaminated with suspended sediments, heavy metals, hydrocarbons, nutrients, and pathogens (Eriksson et al 2007; Joshi and Balasubramanian 2010; Barbosa et al 2012).

A major challenge for stormwater management in the 21st century is to develop strategies that encompass increasing impervious surfaces from the expansion of urbanized areas, while maintaining the health of the watershed and fulfilling the governmental requirements for stormwater quality (Barbu et al

2009). As a response, low impact development (LID) planning and related best management practices (BMPs) have been used recently to reduce the adverse effects of urbanization on surface water. LID BMPs collect, infiltrate, treat urban runoff, and increase recharge to local aquifers (SFPUC 2010, Department of Environmental Resources 1999, Holman-Dodds et al. 2007). Newcomer et al. (2014) showed that recharge beneath some LID BMPs can be orders of magnitude larger than beneath other urban sources of recharge. Treatment of pollutants in surface waters and groundwater recharge is considered as an advantage of LID BMPs (USEPA 2009; Dietz and Clausen 2005; Lu and Yuan 2011), however few studies have examined the influence of LID BMP design features on geochemical processes that occur in the vadose zone and the implications of these process on urban groundwater quality.

Geochemical processes are likely important controls on the quality of stormwater that infiltrates and eventually becomes recharge. In particular, reduction/oxidation (redox) processes can: (i) affect the mobility and availability of organic micro-pollutants such as pharmaceutically-active compounds, pesticides, organic halogens, and other halogenated organic compounds; (ii) affect the fate and mobility of potentially toxic metals associated with naturally occurring aquifer material; (iii) contribute to the degradation or preservation of anthropogenic contaminants; and (iv) generate undesirable byproducts such as

dissolved manganese (Mn^{2+}), ferrous iron (Fe^{2+}), hydrogen sulfide (H_2S), and methane (CH_4) (Korom 1992; Cao et al. 2001; McMahon et al. 2009; Ramesh Kumar and Riyazuddin 2012). Therefore, characterizing and quantifying redox conditions beneath LID BMPs is important to better understand the influence of LID on urban groundwater quality.

1.2.Low Impact Development

LID is a stormwater management and planning strategy with a goal of mimicking the predevelopment hydrologic regime through the use of design techniques to create a functionally hydrologic landscape (U.S. Environmental Protection Agency 2000). LID design techniques include microscale and spatially distributed BMPs such as bioretention-swales, rain-gardens, and infiltration trenches (Department of Environmental Resources 1999). LID BMPs are constructed based on a combination of site characteristics such as land use, soil texture, drainage area, and key hydrological functions such as precipitation, infiltration, surface runoff, and groundwater recharge (Department of Environmental Resources 1999; U.S. Environmental Protection Agency 2000, SFPUC, 2009).

1.3.Reduction/Oxidation (Redox)

In a previous study, Datry et al. (2004) reported that redox conditions in soils and groundwater are affected by the transit and residence times of infiltrating water in the vadose zone beneath a stormwater infiltration basin. Similarly, von Rohr et al. (2014) found that the hydraulic residence time, which is determined by the infiltration rate, may influence the redox conditions during riverbank filtration. Greskowiak et al. (2005) showed that the hydraulic regime immediately below an artificial recharge pond near Lake Tegel, Germany is characterized by cyclic changes between saturated and unsaturated conditions that influence the redox conditions.

The saturation conditions in soils and groundwater influence microbial activity and, in turn, redox conditions because most redox processes are microbially catalyzed (Thomas et al. 2009; McMahon 2009). Additionally, microbial activity is temperature dependent and thus a function of diel and seasonal cycles (Datry et al 2004; Massmann et al 2006). Datry et al. (2004) reported that microbial respiration in an infiltration basin was stimulated by the increase in temperature, thereby leading to higher oxygen deficit in summer, whereas cold winter stormwater slightly re-oxygenated groundwater. During periods of cooler soil temperatures, from November through March, saturated soils take longer to become reducing (Vaughan et al 2007).

Molecular oxygen acts as the preferred electron acceptor through aerobic respiration because it is the most energetically favorable reaction (Tesoriero and Puckett 2011). If the supply of O_2 is consumed or absent, alternative electron acceptors are used by microbes. After O_2 , the descending sequential order of acceptor preferences is nitrate (NO_3^-), manganese (IV) (Mn^{4+}), ferric iron (Fe^{3+}), sulfate (SO_4^{2-}), and finally carbon dioxide (CO_2). This order of preferential electron acceptor utilization— $O_2 > NO_3^- > Mn^{4+} > Fe^{3+} > SO_4^{2-} > CO_2$ —is referred to as the ecological succession of terminal electron-accepting processes (Fiedler et al. 2007; McMahon and Chapelle 2008; McMahon 2009).

For the purpose of this study, threshold concentrations of dissolved oxygen (DO) will be used to identify general redox conditions and processes following a framework developed by McMahon and Chapelle (2008). Under this framework, oxic conditions are present when observed DO concentrations are ≥ 0.5 mg/L and thus O_2 reduction is the predominant redox process. Anoxic conditions are present when observed DO concentrations are < 0.5 mg/L.

The rate of O_2 reduction has a significant influence on the susceptibility of aquifers to many contaminants (Tesoriero and Puckett 2011). Therefore, quantifying the rate of O_2 reduction in the gravel bed of the LID infiltration trench is an important indication of the progression of redox reactions in the infiltration trench and sub-soils beneath. Under anoxic conditions, NO_3^- is the preferred

electron acceptor and NO_3^- reduction (denitrification) is the predominant redox process when NO_3^- concentrations are $>0.5 \text{ mg/L}$ (McMahon and Chapelle 2008). Understanding when NO_3^- reduction occurs beneath LID BMPs is important because urban stormwater often contains elevated nutrients, including NO_3^- . NO_3^- is also the most ubiquitous contaminant of groundwater worldwide (Spalding and Exner, 1993), and NO_3^- reduction can release the greenhouse gas nitrous oxide and pose well-known ecological and human-health risks (Fan and Steinberg 1996; Galloway et al. 2003). After NO_3^- has been reduced, redox processes may continue along the ecological succession of terminal electron-accepting processes.

1.4.Objectives and Hypothesis

The primary objective of this study is to characterize how BMP design features affect redox conditions in the vadose zone and groundwater beneath a LID infiltration trench. DO is a function of saturation (%) and water temperature ($^{\circ}\text{C}$). Therefore, this study describes the relation between saturation (%) and water temperature ($^{\circ}\text{C}$) within the gravel of the infiltration trench and subsurface DO concentrations. This study is important because it helps inform how LID BMPs can be best engineered to optimize the saturation and water temperature within a desired range of DO concentrations in the infiltrating water. I hypothesize that the DO concentrations in water beneath the LID infiltration trench vary inversely

with saturation (%) of gravel. I expect to find that DO concentration decrease soon after the gravel reaches 100% or partial saturation, resulting in anoxic conditions within hours to days after rain-events. I also hypothesize that there is an inverse relation between DO concentrations and water temperature in the LID infiltration trench, with lower DO concentrations in water with higher temperatures due to increased microbial respiration and the known inverse relation between water temperature and DO.

The second objective is to characterize the magnitude and duration of fluctuations in DO concentrations in response to changes in saturation of gravel and water temperature in the infiltration trench. As part of this objective, I calculated the O₂ reduction rates in the gravel of the LID BMP. I hypothesize that infiltrated oxic stormwater will reach anoxic conditions within hours to days of the beginning of the storm event. However, I expect relatively short durations (hours to days) of anoxic conditions in the LID feature. I expect redox conditions to return relatively quickly to oxic conditions after the end of the rain event as a result of rapid infiltration rates and drying of the subsurface or by re-oxygenation with oxic stormwater runoff.

2.0 Methods

2.1. Study Area

The study area is a recently installed (2009) and instrumented (2011) BMP infiltration trench site at the San Francisco State University (SFSU) LID research network, within the city of San Francisco, California, USA (Figure 1). The Westside Basin aquifer (104 km²) is located beneath the study site and is part of the regionally important California Coastal Basin aquifers (Figure 1). The Westside Basin aquifer system has a shallow (< 30 m below sea level), unconfined aquifer and two deeper confined aquifers, and is bounded in the north and south by Franciscan Complex bedrock ((Clifton et al., 1988; Nzewi et al., 2010). The aquifer sediments include coastal deposits of sand, silt, mud, gravel, and peat from the Merced and Colma Formations (Nzewi et al., 2010).

The BMP infiltration trench was installed in 2009 and is approximately 11 m² (0.90 m x 12 m) in area and located in the center of a vegetated depression that collects runoff from an impervious bike path, parking lot, and surrounding roof tops with an effective drainage area of 430 m² (Figure 2). The gravel trench has a maximum storage capacity of approximately 33 m³ assuming a gravel porosity of 0.35. The design of the infiltration trench generally follows the volume-based sizing method and a goal of 80% stormwater volume capture (CASQA, 2003) for

one-hour, six-hour, and 24-hour precipitation events (design storms) with a two-year return interval.

In a previous study on this site, soil samples from this site were collected and analyzed. Soil textural class and hydraulic properties, for cores collected at the infiltration trench are shown in Table 1 (Newcomer et al. 2014).

2.2. Saturation of Gravel

I evaluated saturation of the gravel trench based on hourly precipitation during the period of field observation (July 2012 – June 2014). Here, saturation (%) of gravel refers to the ratio of water level [L] in the gravel to total depth of the gravel [L] at each well. Figure 3 shows a cross section of the infiltration trench with gravel depths relative to each of the wells. I calculated saturation (%) using equation 1:

$$\text{Saturation (\%)} = \frac{\text{Observed Water Level}}{\text{Depth of Gravel}} \times 100 \quad \text{eq.1}$$

where the observed water level [L] is an average of water levels for each well during an hourly time interval. Once 100% saturation of the gravel trench has been reached, the excess stormwater is assumed to overflow into the stormwater system. Total depth of stormwater collected in the gravel is assumed to infiltrate and eventually become recharge. I assume that loss due to evapotranspiration (ET) is negligible because the gravel is not vegetated.

The duration of saturation (%) in the gravel trench is defined as the length of time (reported as either hours or days) when water levels were elevated above the pre-rainfall event water levels. I estimated the duration of saturation using observed timeseries of water levels and precipitation.

2.3. Vadose Zone Data Collection

The infiltration trench site is instrumented with five Decagon 5TM soil temperature and moisture sensors, five Decagon MPS-1 matric potential sensors, and one Decagon G3 drain gauge (passive capillary lysimeter), which continuously record measurements at a two-minute interval to detect event-based changes in drainage beneath the gravel in the vadose zone (Figure 4).

Additionally, one Decagon ECRN-100 rain gauge, one Solinst Inc. barometer, and three piezometers with Solinst Inc. pressure transducers were installed at the infiltration trench site (Figure 4). The pressure transducers at the three piezometers measure water level, temperature, and conductivity. A fourth piezometer was installed 2.13 m below land surface beneath the infiltration site to manually collect water level. Each piezometer was constructed of pvc pipe with a slotted screen. An offset correction for observed sensor drift was applied to water levels from wells 1 and 2, following methods recommended by Solinst technical bulletin (Solinst Inc. 2014).

MiniDot oxygen loggers (PME, 2012) were installed in the infiltration trench on November 11, 2013 to measure DO concentrations along the flow path in the infiltration trench. The miniDot oxygen loggers were installed in 5 cm (2 inch) diameter piezometers near wells 1 and 3 (Figures 5a and 5b). These loggers were programmed to make measurements at two-minute intervals, which is consistent with the sampling frequency of the other field instruments. For the DO sensors in the miniDot oxygen loggers to be in contact with water, water levels in the 5 cm piezometers near wells 1 and 3 have to be at least 26 cm and 34 cm above the base of the gravel, respectively. The miniDot oxygen loggers measure and record DO concentrations with an accuracy of $\pm 5\%$ and temperature to $\pm 0.1\text{ }^{\circ}\text{C}$ (PME, 2012).

2.4. Precipitation

Historical hourly and daily precipitation data from the San Francisco, Downtown station (Station ID: 047772) were evaluated for the entire data collection period at the LID BMP (July 2012–June 2014) (NOAA NCDC, 2014). Hourly precipitation data were obtained in GMT time zone and were converted to San Francisco local time. Hourly precipitation time series were compared to the water level, temperature, conductivity time series for the entire collection period and with DO concentrations between February 22, 2014 and June 30, 2014. The shorter collection period of DO concentrations reflects the fact that the miniDot

oxygen loggers were installed at a later time than the LTC loggers. Hourly and daily precipitation data were used to develop hourly and daily runoff volumes for the entire data collection period.

Precipitation frequency estimates with 90% confidence intervals for the San Francisco, Downtown station are shown in Table 2 (NOAA NWS, 2014). Depth-duration-frequency curve for this station were developed using the precipitation frequency estimates data from NOAA's precipitation data server (NOAA NWS, 2014) and are shown in Figure 6. Annual exceedance probability (AEP) (Figure 7) for the SF downtown station precipitation depths was calculated based on the Langbein's formula (Langbein, 1949) that transforms a partial duration series (PDS)-based average recurrence interval (ARI) (NOAA NWS 2014) to an annual exceedance probability (AEP).

$$AEP = 1 - e^{-\frac{1}{ARI}} \quad \text{eq.2}$$

AEP is defined as the probability associated with exceeding a given amount in any given year once or more than once; the inverse of AEP provides a measure of the average time between years (and not events) in which a particular value is exceeded at least once (NOAA Atlas 14, 2011).

2.5. Runoff

The infiltration trench collects runoff from an effective drainage area of 430 m² that includes an impervious bike path, parking lot, and surrounding roof tops. Daily and hourly runoff to the infiltration trench was calculated for the period 2012 to 2014 using the TR-55 SCS curve number method (Pazawash 2011). A curve number of 98, representing impermeable surfaces such as roofs and pavement was applied to the impermeable surfaces draining to the trench. Runoff depth was calculated using equations 3 and 4 shown below.

$$R = \frac{(P - 0.2 S)^2}{(P + 0.8 S)} \quad \text{eq.3}$$

And

$$S = \frac{1000}{CN} - 10 \quad \text{eq.4}$$

where R is the runoff [L T⁻¹], P is the precipitation [L T⁻¹], S is the maximum retention, and CN is the composite curve number (unitless). Runoff volumes (m³) were calculated by multiplying daily or hourly runoff depths by the effective drainage area of 430 m².

2.6. Rate of O₂ Reduction

The rate of O₂ reduction in the gravel bed in the infiltration trench was evaluated by relating measured DO concentrations to the time since stormwater infiltrated into the gravel (elapsed time) following the approach described by McMahon et al. (2008) and Tesoriero and Puckett (2011). Elapsed time is defined here as the duration (minutes) since beginning of a rain event, until the lowest DO concentrations measured during and after the rain event. Zero-order reaction rates were estimated from changes in concentration of DO with elapsed time using the following equation:

$$-K_0 = \frac{\Delta(C-C_0)}{\Delta t} \quad \text{eq. 5}$$

where $-K_0$ is the rate (mg/L min) for zero-order reaction kinetics, C is the concentration of DO at the time of interest (mg/L), C_0 is the initial concentration of DO (mg/L), and Δt is the elapsed time (min). Zero-order rates were determined by fitting a linear regression curve to a plot of DO versus elapsed time. It should be noted that large errors in zero-order rates are more likely to occur when reactant concentrations become limiting (Bekins et al. 1998).

2.7. LID Oxygen Demand Rate

The LID oxygen demand (LIDOD) rate is defined here the rate at which dissolved oxygen (DO) is consumed by microbial respiration processes occurring

in the gravel bed in the infiltration trench. I calculated the LIDOD using a modified method from Kenny et al. (2009) and Wilson (2013) under three rain events that occurred during the period of field observation of DO. The measured DO concentrations for wells 1 and 3 were plotted as a function of elapsed time, resulting in a DO depletion curve. Elapsed time for each rain event was considered to be between the beginnings of rain events until the lowest DO concentrations measured before recovery of DO levels to pre-event conditions. The slope of the linear part of the oxygen-depletion curve was determined through linear regression and used to calculate the LIDOD rate using equation 6:

$$LIDOD_T = \frac{V_{water}}{V_{trench}} \times b \quad \text{eq. 6}$$

where $LIDOD_T$ is the LID oxygen demand rate ($\text{mg}/\text{m}^3 \text{ min}$) at water temperature T ; V_{water} is the volume of water in the gravel (L); V_{trench} is the maximum volume capacity of infiltration trench (m^3); and b is the slope of the oxygen-depletion curve for each storm ($\text{mg}/\text{L min}$). In order to standardize DO measurements among different rain events and temperatures, the measured LIDOD rates are adjusted to 20°C using a standard van't Hoff equation in equation 7 (Heckathorn and Gibbs, 2010):

$$LIDOD_{20} = LIDOD_T / 1.065^{(T-20)} \quad \text{eq. 7}$$

where $LIDOD_{20}$ is the LID oxygen demand rate ($\text{mg}/\text{m}^3 \text{ min}$) at 20°C , and T is the water temperature ($^\circ\text{C}$).

Since DO concentrations and temperature were measured at a 2-minute interval, the $LIDOD_T$ and the $LIDOD_{20}$ rate were calculated every 2-minutes for each rain event for wells 1 and 3. Volume of water in the gravel was calculated based on an average water level from wells 1 and 3. An average of the calculated $LIDOD_{20}$ rates for all rain events for both wells was calculated and this average represents the $LIDOD_{20}$ for the entire infiltration trench.

3.0 Results

This section presents hydrologic and geochemical time series and analyses of field data and stormwater storage in the infiltration trench.

3.1. Precipitation

During the period of field observation period (July 2012–June 2014), all of the hourly and daily precipitation were below the 2–5 year design storm values ($<14.99 \text{ mm}$ and $<60 \text{ mm}$ respectively in Table 2). The maximum hourly and daily precipitation was 12.7 mm and 35.4 mm (Figure 8), respectively.

3.2. Water Levels

Time series of water level in piezometers (height above sensor) for the entire period of field observation for each well are shown in Figures 9b, 10b, and 11b. The observed water levels in the infiltration trench fluctuate as a response to the volume of stormwater received during rain events through the inlet drain pipe (Figure 3) and from direct precipitation. Figure 12 shows water level response to a range of rainfall intensities that occurred between November 20 – December 05, 2012 for wells 1, 2, and 3. Maximum water levels for wells 1, 2, and 3 are 93.8 cm, 81.1 cm, and 95.3 cm respectively. The maximum water levels occurred during a rain-event on December 02, 2012 that had a maximum hourly precipitation of 12.7 mm, 26.9 mm of total daily precipitation (over 6 hours), and 9.26 m³ of daily runoff to the infiltration trench. Water levels in all three wells increased rapidly within less than an hour of the beginning of the rain for all the rain events that occurred between November 20 and December 05, 2012. Subsequent rain events with short intervals of dry periods (less than 24 hours), such as between November 29 and December 02, 2012, maintained water levels at higher than pre-event levels throughout the events (Figure 12). Conversely, water levels returned to pre-event levels sooner for the three wells after the end of a lower intensity rain event (with no subsequent rainfall). For example, it took

about 3.8 days for water levels to recover due to the rain event on November 20 – 21, 2012.

Water levels decline along the flow path within the LID feature, first in well 1 (closest to the inlet pipe) (Figure 12a) and then in well 2 (mid-way along the LID feature) (Figure 12b). However, higher water levels were observed at well 3 (farthest from inlet pipe) (Figure 12c) than at wells 1 and 2. Stormwater input during the rain events shown in Figure 12, resulted in ponding in the LID feature as evident by water level peaks exceeding ground surface line for all three wells.

3.3. Saturation of Gravel

Timeseries of precipitation and hourly % saturation of gravel at each well for rain events that occurred during the rainy season (November to March) of 2013 and 2014 are shown in Figures 13 and 14, respectively. During this period, the water levels were present and saturation was always greater than 0%. Minimum hourly% saturation for these two rainy seasons are 1.57 % in well 1, 0.005% in well 2, and 0.009% in well 3.

Rain events during this period resulted in substantial increase in % saturation. During rain events, saturation of gravel is noticeably higher in well 1 than in wells 2 and 3 (Figure 13). However, saturation near well 3 is only slightly greater than in well 2. For example, the response in % saturation in gravel to input stormwater

from rain event on November 28, 2012 (Figure 13a) resulted in an increase in saturation in well 1 to 62% within 11 minutes after the beginning of the rain. Whereas, the saturation increased to 40% in well 2 and to 52% in well 3 within an hour after the beginning of the rain event. Rain events that occurred during November 28 – December 05, 2012 (Figure 13a) resulted in a maximum of 125% for well 1, 107 % for well 2, and 107% for well 3. Subsequent rain events with short dry periods in between (< 24 hours), resulted in fluctuations in saturation of gravel that resemble fluctuations in water levels (Figure 12) that I observed during the same rain events.

The duration of saturation typically lasted for several days after the end of the rain events and depended on the intensity and duration of rain events (Figures 13 and 14). The maximum duration that the infiltration trench was saturated above minimum values was about 12–14 days for all three wells (for saturation levels to go back to pre-event conditions). I observed maximum duration of saturation in gravel during subsequent rain events that occurred during December 21-29, 2012 (Figure 13b) and February 26 – March 05, 2014 (Figure 14). Lower intensity rain events generated less duration of saturation, as in a rain event that occurred on February 02, 2014 (Figure 14a) where it took about 2-3 days for saturation levels to go back to pre-event conditions for all three wells. The vast majority of

stormwater collected in the gravel at the three wells is assumed to infiltrate into the sub-soils beneath the infiltration trench.

3.4. Water Temperature

Time series of water temperatures for the period of field observation July 2012 – June 2014 for each well are shown in Figures 9c, 10c, and 11c. Observed water temperatures show variation before and after rain events during the rainy seasons of 2013 and 2014. Detailed timeseries for rain events and water temperature that occurred between October 31 – November 01, 2012; December 20 – 28, 2012; and March 30 – April 02, 2013 for wells 1, 2, and 3 are shown in Figure 15. These rain events resulted in total runoff of 1.17 m³ (over 2 days), 27.6 m³ (over 6 days), and 1.4 m³ (over 2 days) into the LID trench, respectively. Infiltrated stormwater both increased and decreased the temperature of existing water in the LID trench, which was a function of the relative difference between the temperature of the infiltrating water and that water already in the trench. Responses in the water temperature were generally observed within 1 hour after the beginning of each rain event. The Oct – Nov, 2012 event resulted in a sharp increase in water temperature from 13.85°C to 14.75°C within 7 hours for well 1, from 13.93 °C to 14.52 °C within 8 hours for well 2, and from 13.79 °C to 13.97 °C within 9 hours for well 3 (Figure 15). While rain continued for two more

hours after peak water temperature, there was a gradual decline in water temperature until reaching the approximate pre-event temperatures.

The rain event on Dec 21, 2012 resulted in a decrease in water temperature from 11.3°C to 10.39°C for well 1, 10.91 °C to 10.24 °C for well 2, and from 11.58 °C to 11.13 °C for well 3. However, subsequent continuous rain on Dec 22 and 23, 2012 resulted in a gradual increase in water temperatures for well 1 and fluctuations in water temperatures (increase and decrease) for wells 2 and 3 were observed.

Rain events from March 30 – April 02, 2013 resulted in an increase in water temperature with input of infiltrated stormwater for all three wells (Figure 15). On March 30, 2013 water temperatures increase from 11.39 °C to 13.7 °C for well 1, from 11.75 °C to 12.67°C for well 2, and from 11.15 °C to 11.23 °C for well 3. However, the pattern of response in water temperature for well 3 are different than wells 1 and 2 for some of these events. Figure 15 shows lower peaks for water temperature at wells 2 and 3 than well 1 for rain events on October – November 2012 and March-April 2013. Increases in water temperatures for well 3 are noticeably more gradual and dampened.

3.5. Specific Conductance

Time series of specific conductance ($\mu\text{S}/\text{cm}$) for the period of field observation July 2012 – June 2014 for each well are shown in Figures 9d, 10d, and 11d. Specific conductance demonstrates a marked decrease with instant increase in water level as the LID trench was replenished with stormwater during rainfall events. These observations are consistent with previous studies. Datry (2004) found that inflow stormwater into a stormwater infiltration basin resulted in a sharp decrease in specific conductance in the infiltration bed. Appleyard (1993) has demonstrated similar results where stormwater recharge through infiltration basins receiving runoff from large impervious catchments of the Perth metropolitan area, Australia, caused a marked reduction in total dissolved salts to depths of more than 10 m below the groundwater table.

Rain event on November 20, 2012 resulted in a decrease in specific conductance within 1 hour after beginning of the rain from 323 $\mu\text{S}/\text{cm}$ to 0.5 $\mu\text{S}/\text{cm}$ for well 1 (Figure 16a), 226.7 $\mu\text{S}/\text{cm}$ to 0 $\mu\text{S}/\text{cm}$ for well 2 (Figure 16b), and 187 $\mu\text{S}/\text{cm}$ to 176.6 $\mu\text{S}/\text{cm}$ for well 3 (Figure 16c). Following this reduction, specific conductance gradually starts increasing, and with absence of stormwater infiltration, specific conductance returns to pre-event conditions within 2-4 days for wells 1 and 2, and even above pre-event conditions for well 3.

Rain events that occurred from November 28 – December 02, 2012 (Figure 16a, 16b, and 16c) resulted in fluctuations in specific conductance with change in water levels. Moreover, specific conductance stayed relatively lower than pre-event conditions throughout. Similar to water temperature response in well 3, specific conductance reduction is dampened for well 3 compared to wells 1 and 2.

3.6. Dissolved Oxygen

DO concentrations that were measured continuously by the miniDot loggers in the LID trench for the period of field observation (February – July 2014) for well 1 and 3 are shown in Figures 17a and 17b, respectively. DO concentrations are measured in mg/L and % saturation at depths 45 cm and 54 cm for wells 1 and 3, respectively. Changes in DO concentrations during rainfall events of increasing intensity are shown in Figures 18a and 18b for well 1, and in Figures 19a and 19b for well 3. The rain event on February 26, 2014 had a maximum hourly precipitation of 5.84 mm and 7.79 m³ of daily runoff generated from 23.4 mm of total precipitation (over span of 16 hours). The rain event on March 03–04, 2014 had a maximum hourly precipitation of 1.27 mm and a combined total runoff of 0.87 m³ generated from 7.1 mm of total precipitation (over span of 13 hours).

DO concentrations in the gravel trench decreased with input of stormwater when pre-event conditions in the gravel trench were oxic (Figures 18 and 19).

However, DO concentrations increased with input of stormwater when DO concentrations in the gravel were anoxic or at lower concentrations than DO in input stormwater. Measured DO concentrations in stormwater from the inlet pipe during rain event on February 26, 2014 ranged between 6.86 – 8.25 mg/L. These concentrations fall within range of measured DO concentrations in stormwater from previous studies of 6 to 9.90 mg/L (Datry et al 2004; Sansalone et al 2005)

DO concentration in the gravel trench started to decline within less than an hour after the beginning of the rain for each event. During the rain event on February 26, 2014, DO concentrations declined from 9.22 to 3.40 mg/L within one day since beginning of rain for well 1 (Figure 18a). A subsequent smaller event on February 27, 2012, slightly increased DO in well 1, but then DO rapidly decreased to anoxic conditions (<0.5 mg/L). Subsequent rain events occurring from February 28 – March 02, 2014 resulted in fluctuations from anoxic to oxic conditions where DO stayed below 4 mg/L and was consumed rapidly. Fluctuations in DO concentrations caused by the February 28 – March 02, 2012 events coincide with fluctuations in water levels in the gravel trench as a response to input stormwater (Figure 18a). During these rain events, anoxic conditions prevailed only during a short period (15 hours). Return to pre-event oxic conditions was as a result of 1) replenishment with oxic stormwater over short time intervals or 2) reduced water levels in piezometer below 29 cm (minimum

required water level in 2" piezometer near well 1 for DO sensor to be in contact with water).

Well 3 (Figure 19a) shows similar response as in well 1 in DO concentrations during the February 26, 2012 rain event; DO declined from 10.34 to 1.40 mg/L within 1.5 days since beginning of rain. Subsequent rain events occurring on February 28 – March 02, 2012 result in a larger increase in DO (5.26 mg/L) and less fluctuations (only one peak) when compared to DO response in well 1 to the same rain event. DO declined rapidly and reached anoxic conditions (<0.5 mg/L) within 1.3 day after beginning of rain on February 28, 2012. Anoxic conditions prevailed for almost 2 days which is a longer period than observed in well 1. Return to highly oxidic conditions (~ 10 mg/L) after end of rain events was due to reduced water levels in piezometer below 34 cm (minimum required water level in 2" piezometer near well 3 for DO sensor to be in contact with water).

The March 03–04, 2012 rain event was preceded with a dry period of more than 24 hours. For well 1, DO concentrations were highly oxidic (>8 mg/L), but declined with input of stormwater from 8.3 to 1.8 mg/L within approximately 1 day since beginning of rain (Figure 18b). A similar scenario followed for the rain event on March 05–06, 201, where DO concentrations declined from 9.10 to 1.12 mg/L within 1.8 days since beginning of rain. DO concentrations never reached

anoxic conditions and returned to pre-event concentrations due to reduced water levels in piezometer below 29 cm.

For well 3 (Figure 19b), input stormwater from the March 03–04, 2012 event resulted in a decline in DO from 10.0 to 1.50 mg/L within 1.8 days since beginning of rain. Rain event that occurred on March 05–06, 2012 resulted in a decline in DO from 10.2 to 3.10 mg/L within 1.7 days since the beginning of rain. Similar to well 1, DO concentrations never reached anoxic conditions and returned to pre-event concentrations due to reduced water levels in piezometer below 34 cm.

3.7. Rate of O₂ Reduction

Rate of O₂ reduction for wells 1 and 3 were estimated for 6 rain events during the period (February – June, 2014). O₂ reduction plots (Figures 20 and 21) show a linear relation with time from the beginning of the rain event to the lowest DO values during that event. The linear fit for these plots shows a narrow range of O₂ reduction zero-order rates: 0.102 – 0.004 mg/L min for well 1 and 0.002 – 0.005 mg/L min for well 3. An O₂ reduction rate for the entire infiltration rate was calculated based on an average of all the zero-order rates from both wells, resulting in a value of 0.003 mg/L min, which is equivalent to 0.179 mg/L hour. Summary of the zero-order rates for both wells are shown in Table 3.

3.8. LID Oxygen Demand Rate (LIDOD)

The measured DO concentrations for wells 1 and 3 were plotted as a function of elapsed time (in minutes) beginning from the start of the rain event until the lowest DO concentrations measured before recovery of DO levels to pre-event conditions (Figures 22a and 22b). The slope of the best-fit regression line for each curve was calculated; these slopes are used to estimate the $LIDOD_T$ and $LIDOD_{20}$ for each event, which are summarized in Table 4. The range of $LIDOD_T$ for well 1 is $1.48 - 2.49 \text{ mg/m}^3 \text{ min}$, and $1.80 - 1.83 \text{ mg/m}^3 \text{ min}$ for well 3. The $LIDOD_T$ were converted to $LIDOD_{20}$, which ranged between 2.23 and $3.59 \text{ mg/m}^3 \text{ min}$ for well 1 and 2.80 and $2.81 \text{ mg/m}^3 \text{ min}$ for well 3. The $LIDOD_{20}$ value for the entire infiltration trench is based on an average of the $LIDOD_{20}$ for all events from both wells, and is estimated to be $2.71 \text{ mg/m}^3 \text{ min}$.

4.0 Discussion

5.1. Dynamics of Water Level, Temperature and Conductivity in LID Trench under Stormwater Runoff Influence

Precipitation events throughout the period of field observation (2012–2014) resulted in sharp and substantial increases in water levels in all three wells (Figures 9b, 10b, and 11b). The response in water levels in all three wells occurred within a short time-lag (less than an hour) between the beginning of rain

event and the first increase in water levels above pre-event values. These water levels are measured at depths 74 cm below ground surface (bls) for wells 1 and 2, and 88 cm bls for well 3. This fast response to precipitation events indicates relatively high infiltration rates in the LID infiltration trench, which allows to capture most of the stormwater runoff and convert into recharge. The recharge rates beneath the LID infiltration trench were estimated to be about 1,750 to 3,710 mm yr⁻¹ (Newcomer et al. 2014). Elevated water levels were maintained for longer periods under subsequent rain events with < 24 hours short period between rain episodes than during shorter duration rain events (Figure 12). This dissimilarity is most likely a result of further decreased infiltration rates due to increased saturation % in the gravel bed. The infiltration rate beneath the trench is a function of the saturated hydraulic conductivity value for the soil beneath the gravel. As soil moisture increases, the infiltration rate gradually decreases with time and approaches the value of the saturated conductivity of the soil (Brady and Weil 2002).

Evidence of spatial and flow geometry variation in the LID trench is demonstrated by different water levels and saturation % under same rain event for the three wells. Water levels and saturation % are generally higher near well 1 (closer to the inlet pipe) than well 2 (Figures 12, 13, and 14) as a result of well 1 receiving more water sooner due to proximity to the inlet pipe causing ponding

momentarily as water infiltrates downward or laterally in infiltration trench. However, water levels at well 3 (located farthest from inlet pipe) are slightly higher than wells 1 and 2. Well 3 is located near the cement overflow drain structure at the downstream end of the infiltration trench. The overflow drain most likely acts as an impermeable surface which inhibits lateral water flow near well 3. Saturation % in well 3 is higher than well 2, also due to the impermeable cement structure. When stormwater input rate (runoff) exceeded the maximum storage capacity of the LID trench, the excess stormwater accumulated at the surface as ponding. All rain events that caused ponding in the LID trench during the 2012–2014 period of field observation are below the 2–5 year design storm values (<60 mm).

Measured water temperatures in the infiltration trench fluctuated depending on the temperature of incoming stormwater runoff. Mixing of existing water in the gravel with colder and warmer stormwater decreased and increased water temperature in the gravel, respectively (Figure 15). Increases in water temperatures decline along the flow path in the infiltration trench from wells 1 to 3. Moreover, the response is more gradual and dampened for well 3. Spatial variation in temperature response between the three wells is influenced by the increasingly cooled down infiltrated stormwater temperature by lateral flow in the

gravel until it reached wells 2 and 3 and (or) longer time of vertical flow near well 3 where gravel is deeper than wells 1 and 2.

Stormwater input to the water table resulted in a low-salinity plume in the gravel bed. These results are similar to findings from a previous study where inflow stormwater into a stormwater infiltration basin resulted in a decrease in specific conductance in the infiltration bed (Datry et al 2004). Similar to water levels and temperature, response in specific conductance to infiltrating stormwater is within a short time lag. This finding may be the result of dilution by infiltrating stormwater.

5.2. DO Dynamics in Response to Saturation of Gravel

Input stormwater into the infiltration trench resulted in a rapid and substantial increase in % saturation in gravel. Saturation in gravel column near wells 1 and 3 has to be $\geq 39\%$ for the DO sensors to be in contact with infiltrated water and to measure fluctuations in concentrations (Figure 23). Therefore, DO concentrations are measured at depths 45 cm and 54 cm below ground surface for wells 1 and 3, respectively. When the % saturation in gravel is below 39%, DO concentrations detected by the sensors show highly oxenic conditions (> 8 mg/L). Once the saturation in gravel crossed the 39% threshold, DO concentrations started declining rapidly, reaching anoxic conditions (< 0.5 mg/L) during some rain events (Figure 23). The time lag is very short between the pulses of

increased saturation and decreased DO concentration. These results indicate that DO dynamics in the gravel bed are influenced by hydraulic conditions in the gravel with an apparent inverse relation between the duration of % saturation in the gravel and DO concentrations (described in Section 5.3), and that DO is quickly consumed, which is likely caused by microbial respiration activities in the gravel.

Stormwater provides the infiltration trench with organic matter (Datry et al 2003; Vaughan et al 2009) that can induce microbial respiration reactions in the gravel bed. Furthermore, observed water temperatures for the period of field observation of DO (February – June, 2014) range between (12 °C – 23 °C) (Figure 20), which are above the benchmark temperature referred to as the biological zero (5 °C). Generally, microbial activities virtually cease below the biological zero value (Brady and Weil 2002).

Input stormwater into the infiltration trench, induced a decrease in DO from oxic conditions (> 8 mg/L) to low oxic conditions (0.5 – 2 mg/L) and anoxic conditions (<0.5 mg/L) (Figure 17). Fischer et al. (2003) detected severe DO depletion (i.e., DO < 0.5 mg/L) below several infiltration basins in southern New Jersey, USA. In contrast, Datry et al. (2004) demonstrated that stormwater infiltration induced only a moderate (2 mg/L) increase in DO concentration of groundwater during rains under similar temperature conditions as the present

study. The only exception to the decreasing pattern of DO concentrations with input stormwater, occurred during the February 28 – March 02, 2014 rain events (Figures 18 and 19). These events resulted in fluctuations from anoxic to oxic conditions where DO stayed below 4 mg/L. Therefore, incoming oxic stormwater increased DO slightly but was consumed rapidly as expected and reached anoxic conditions (< 0.5 mg/L).

Temporal changes in DO concentrations during rain events (shown in Figures 21 and 22) show a relatively quick consumption of DO (hours to days). The onset of DO consumption is noticeable within less than an hour from the beginning of all rain events. The decline in DO from oxic conditions (> 8 mg/L) to low oxic ($0.5 - 2$ mg/L) took less than 2 days (~ 1.2 days) for wells 1 and 3. Anoxic conditions were reached within a day in well 3 and occurred more often in well 3 than in well 1. Anoxic conditions prevailed only during a short period; 15 hours for well 1 and 2 days for well 3. Return to oxic conditions in the infiltration trench was as a result of 1) replenishment with oxic stormwater over short time intervals or 2) reduced water levels in piezometers below 39% saturation.

5.3. DO Dynamics in Response to Duration of Saturation in Gravel

DO dynamics in the gravel bed show some variation based on the duration of saturation in gravel (standing water) as shown in Figures 23a and 23b for well 1 and well 3, respectively. These plots clearly demonstrate that DO concentrations reach

lower levels with longer durations of saturation for both wells. Summary of the rain events, durations of saturations, and DO concentrations shown in Figures 23a and 23b, is shown in Tables 5 and 6. Table 5 and 6 show durations of saturation and corresponding DO concentrations for 6 rain events that occurred during the period of field observation for DO for wells 1 and 3, respectively. Maximum values of DO shown in Tables 5 and 6 refer to DO concentrations in the gravel at the time the rain event began, and minimum values refer to the DO concentrations at the end of saturation period where water levels start recovering. Values of duration of % saturation and DO concentrations in Tables 5 and 6 are representative for depths 45 cm (well 1) and 54 cm bls (well 3). Actual lengths of time of saturation in the whole thickness of the gravel bed are longer than durations given in Tables 5 and 6.

The increased saturation due to input stormwater, increased the water content in the gravel bed and in the sub-soils beneath the infiltration trench. In a previous study done on the study site, Newcomer et al. (2014) demonstrated that substantial increases in volumetric water content occur at all depths beneath the infiltration trench in response to precipitation events. Therefore, I expect that the low oxic to anoxic conditions detected at 45 cm and 54 cm bls for the two well will carry on downward through the gravel and probably into the sub-soils beneath.

There is a general trend of lower DO concentrations with increased duration of saturation as shown in Figures 24a and 24b. Figures 24a and 24b show a scatter plot of the durations of saturations for each of the rain events in Tables 5 and 6 vs. average DO and minimum DO for each event for well 1 and well 3, respectively. Scatter plot in Figure 24a for well 1 shows a downward trend (negative slope) between the durations of saturation and DO concentrations for average and minimum values of DO during each event indicating a negative correlation between the two variables. R^2 for the correlation between average and minimum DO values vs. durations of saturation is 0.898 and 0.714. These results indicate that 89.78% and 71.42 % of variation in average DO concentrations and minimum DO concentrations respectively, can be explained by the corresponding duration of saturation at that time.

Scatter plot in Figure 24b for well 3 shows a similar downward trend (negative slope) but lower R^2 values for the correlation between average DO and minimum DO concentrations vs. durations of saturation than well 1 (0.242 and 0.273, respectively). The lower R^2 for well 3 than well 1 are probably correlated to the spatial variation in redox dynamics between well 1 and well 3. Anoxic conditions in well 3 occurred more often and prevailed longer than well 1 (Figure 23b). Therefore, the variation in DO concentrations under different durations of saturation is less apparent than well 1. The spatial variation in redox dynamics

between well 1 and well 3 is a result of 1) distance from inlet pipe; where well 1 (closest to inlet pipe) shows a more immediate response to rain events due to receiving larger amount of stormwater input sooner than well 3, 2) deeper depth at well 3, which allows more time for microbial reactions, hence lower DO concentrations, and 3) inhibited lateral infiltration near well 3 caused by the impermeable cement overflow structure downstream of the infiltration trench.

Duration of saturation is related to the infiltration rate in the infiltration trench, which generally declines as soils becomes more saturated (Brady and Weil 2002) and transitions towards the saturated hydraulic conductivity during ponded conditions. Lower infiltration rates lead to longer residence time of standing water (duration of saturation) in gravel bed and sub-soils underneath. Longer residence time in turn allows for longer water –gravel and –subsoils contact, permitting sufficient time for DO consumption by microbial respiration reactions. Rudolf von Rohr et al. (2014) showed that low infiltration rates enhanced the oxygen consumption leading to anoxic conditions.

5.4. DO Dynamics in Response to Change in Water Temperature

Measured water temperatures in the infiltration trench ranged between 12 and 22 °C during the period of field observation of DO (February – June, 2014). Infiltration of cooler and warmer stormwater, respectively, decreased and increased water temperatures in the infiltration trench. Higher temperatures are

associated with higher microbial activities in soils, therefore higher rates of DO consumption. Vaughan et al. (2009) observed that during periods of cooler soil temperatures saturated soils took longer to become reducing. However, in this present study there is no apparent influence of changes in temperature on DO dynamics in the gravel. For example, the infiltration of warmer stormwater during rain event on March 29, 2014 (16 °C) did not result in lower DO concentrations than infiltration of cooler stormwater during rain events on March 03, 2014 (13.93 °C) and April 04, 2014 (12.62 °C) (Figure 25a).

Statistical analysis (t-test) of 6 rain events sorted as warm and cold based on average temperature during the period of field observation of DO (February – June, 2014) for wells 1 and 3 are shown in Figures 26 and 27, respectively. Cold rain events are assumed to be less than the average temperature, whereas warm rain events are assumed to be higher than the average temperature. These results show there is no statistical difference (t-test) in DO during warm and cold events.

5.5. Rate of O₂ Reduction and Denitrification

The estimated rates of O₂ reduction for wells 1 and 3 are summarized in Table 3. DO concentrations show a linear relation with time (Figures 20 and 21), indicating a zero-order kinetics for the O₂ reduction process in the gravel. The zero-order reduction rates ranged between 0.102 – 0.004 mg/L min for well 1 and 0.002 – 0.005 mg/L min for well 3, resulting in an average O₂ reduction rate of

0.003 mg/L min for the entire infiltration trench. The zero-order O₂ reduction rates are comparable to the rates estimated based on the LIDOD₂₀ method, which yielded an average value of 0.0027 mg/L min for the entire trench.

The estimated O₂ reduction rate for the infiltration trench (0.003 mg/l min) is 2 to 5 orders of magnitude higher than the O₂ reduction rates for groundwater aquifers estimated in previous studies. Tesoriero and Puckett (2011) estimated a range of zero-order O₂ reduction rates of 9.13×10^{-8} to 4.26×10^{-6} mg/L min in 12 study different shallow aquifers in the US, by relating dissolved O₂ concentrations to groundwater age. McMahon et al. (2008) estimated zero-order O₂ reduction rates for 4 principal aquifers in the US that ranged between 3.81×10^{-7} and 1.14×10^{-5} mg/L min.

Higher rates of O₂ reduction in the infiltration trench than in groundwater aquifers are most probably because the infiltration trench is a more oxic flow system than groundwater aquifers. Therefore, there is more readily available DO for the microbes to consume and of the higher source of organic matter from stormwater input into the infiltration trench than in groundwater aquifers (Datry et al 2003). Aerobic respiration rates are expected to be high in aquifers contaminated with organic compounds (Tesoriero and Puckett 2011). Tesoriero and Puckett (2011) indicated the availability of electron donors as the primary factor affecting O₂ reduction rates. In their study, concentrations of dissolved

organic carbon (DOC) were positively correlated with groundwater age at sites with high O₂ reduction rates and negatively correlated at sites with lower rates.

The presence of anoxic conditions in the infiltration trench is advantageous for the occurrence of denitrification (McMahon and Chappelle, 2008; Landon et al. 2011). The rate of O₂ reduction in the infiltration trench is an important indication if denitrification processes are being carried out in the gravel bed in the infiltration trench. Previous studies identified the O₂ concentration threshold required for the onset of denitrification in groundwater aquifers to be generally < 0.5 mg/l (McMahon and Chappelle 2008), but could be of the order of 1 mg/L (Tesoriero and Puckett 2011) and up to 2 mg/L in some aquifers (Bohlke et al. 2002, 2007; McMahon et al. 2004). The estimated rates for O₂ reduction in this study strongly indicate that the redox conditions favorable for denitrification may be present. Based on O₂ reduction rate of 0.003 mg/L min and a maximum initial DO concentration of 10 mg/L, redox conditions in the infiltration trench may reach the lower end of O₂ concentration threshold required for the onset of denitrification <0.5 mg/L in about 2-3 days. And it would take shorter duration < 2 days for redox conditions to reach < 2 mg/L. These results correlate to the results presented in the timeseries plots of DO concentrations during the period of field observation of DO (Figure 23). It should be noted that the time it takes to reach anoxic conditions in the infiltration trench may vary depending on the initial

oxic conditions present at the beginning of the rain event and the duration the infiltration trench is saturated before it starts recovering to pre-event conditions.

5.6. Design of LID BMP

The degree of % saturation in the infiltration trench is controlled by the water levels in the gravel trench, and the levels fluctuate under wet and dry conditions and intensity of rain. The balance between inflows (Rainfall and Runoff) and outflows (Infiltration), storage capacity of the LID trench, and soil properties will determine how saturated and how long the LID trench will be saturated (duration of saturation).

The infiltration trench has a maximum storage capacity of approximately 3 m³, which is based on the dimensions of the gravel bed and a gravel porosity of 0.35. The relative dimensions of the infiltration trench such as the surface area and average gravel depth may play a role in altering and manipulating the redox dynamics beneath the infiltration trench. In order to examine two design scenarios of the infiltration trench with different dimensions, I assume similar storage capacity and the other elements mentioned above that influence the duration of saturation. In order to satisfy the same storage capacity, we would have smaller surface area and deeper gravel depth (design A) compared to larger surface area and shallower gravel depth (design B).

The different infiltration trench designs would have the same % saturation in the gravel under the same rain event, due to similar storage capacity. However, the duration of saturation will be different for design A than design B. In design A, infiltration of stormwater would take longer due to the deeper gravel depth. As a result of slower infiltration, residence time of standing water (duration of saturation) in the gravel bed would be longer. Longer duration of saturation in turn allows for longer stormwater–gravel contact, permitting sufficient time for DO consumption to be carried out by microbial respiration reactions. Therefore, design A may result in more anoxic conditions and longer duration of anoxic conditions. The residence time of infiltrating stormwater in the vadose zone beneath the infiltration trench increases with longer duration of saturation in the gravel. The observed inverse relation between the duration of saturation and DO concentrations in the gravel, is also expected to be present in the vadose zone beneath the infiltration trench. Groundwater anoxification caused by artificial stormwater infiltration is controlled by the residence time of infiltrating stormwater in the vadose zone (Datry et al. 2006).

In contrast, design B will result in faster infiltration of stormwater causing shorter duration of saturation in the gravel and possibly insufficient time of stormwater-gravel contact for microbial respiration reactions. Therefore, redox

conditions may be less anoxic (less consumption of DO) and/or demonstrate shorter durations of anoxic conditions.

Although water temperature during rain events did not reveal any significant influence on redox dynamics in this study, the two different design of LID trench may show a different behavior under the same temperature. The shallower depth in design B may reduce the cooling effect of the gravel and subsoils on the infiltrating stormwater (Dietz and Clausen 2006). Furthermore, the shallower depth may allow more solar radiation to penetrate through the gravel. Both of these effects may result in warmer infiltrating stormwater encouraging higher microbial respiration rates, hence more anoxic conditions (Datry et al 2004; Massmann et al 2006; Vaughan et al 2009).

5.0 Conclusion

The influence of design features of a BMP LID infiltration trench on the dynamics of DO beneath the BMP LID was investigated using field-based continuous data of DO and water levels and temperatures in the infiltration trench. Saturation % of gravel, duration of saturation in gravel, and temperatures of infiltrated stormwater into the LID infiltration trench are influenced by design features of the LID infiltration trench such as surface area and average gravel depth.

The magnitude and duration of fluctuations in DO concentrations in the LID infiltration trench were found to be influenced by hydraulic conditions in the gravel with an apparent inverse relation between the duration of % saturation in the gravel and DO concentrations. DO was quickly consumed and conditions reached anoxic levels within hours to days, which strongly indicates that microbial respiration activities are a limiting factor of DO in the gravel. Anoxic conditions prevailed for a short period of time (maximum of 2 days) and returned relatively quickly to oxic conditions after the end of rain event as a result of rapid infiltration rates and drying of the subsurface or by re-oxygenation with oxic stormwater runoff. Scatter plots of DO concentrations versus duration of saturation for 6 rain events during the monitoring period demonstrated a general negative correlation between the two variables along the flow path in the LID infiltration trench. However, the variation in DO concentrations under different durations of saturation was found to be less apparent downstream of the inlet pipe than upstream. These results are likely due to the spatial variation in redox dynamics between upstream and downstream of the inlet pipe. This spatial variation is a function of distance from inlet pipe and flow geometry in the infiltration trench.

In contrast to findings with duration of saturation, temperature of infiltrated stormwater was not found to exhibit a major influence on redox dynamics in the

infiltration trench. Statistical analysis of different rain events with different temperatures shows no significant difference between warm and cold infiltrated stormwater.

Collected field data were also used to estimate an average O_2 reduction rate for the LID infiltration trench. The estimated O_2 reduction rate for the infiltration trench was found to be 0.003 mg/L min which is 2 to 5 orders of magnitude higher than the O_2 reduction rates for groundwater aquifers estimated in previous studies. Higher rates of O_2 reduction in the infiltration trench than in groundwater aquifers are most probably because the infiltration trench is a more oxic flow system than groundwater aquifers with more readily available DO for the microbes to consume and of the higher source of organic matter from stormwater input into the infiltration trench than in groundwater aquifers (Datry et al 2003). The estimated O_2 reduction rate in this study strongly indicates denitrification processes are promoted within the gravel. Denitrification is the only natural permanent sink for NO_3^- , which is the most ubiquitous contaminant of groundwater resources worldwide [Gurdak and Qi, 2012].

The observed low oxic and anoxic conditions triggered by infiltration of stormwater in the LID infiltration trench are expected to carry on downward through the gravel and probably into the sub-soils beneath and eventually into groundwater. LID BMPs collect, infiltrate, treat urban runoff, and increase

recharge to local aquifers. Therefore, understanding the redox conditions beneath LID BMPs is essential from an urban groundwater management perspective. Altering the design of LID BMPs to manipulate redox processes can be an important tool to minimize groundwater contamination.

6.0 References

- Appleyard SJ (1993) Impact of stormwater infiltration basins on groundwater quality, Perth metropolitan region, Western Australia. *Environ Geol* 21:227–236.
- Barbosa AE, Fernandes JN, David LM (2012) Key issues for sustainable urban stormwater management. *Water Res.*
- Barbu IA, Ballesterro TP, Roseen RM (2009) LID-SWM Practices as a Means of Resilience to Climate Change and Its Effects on Groundwater Recharge. *World Environ. Water Resour. Congr. 2009 SGreat Rivers*. pp 1–10
- Bekins BA, Warren E, Godsy EM (1998) A comparison of zero-order, first-order, and monod biotransformation models. *Ground Water*, VOL. 36, No. 2.
- Brady NC, Weil RR (2002) *The nature and properties of soils*, 13th edn. Prentice Hall.
- Böhlke JK, Wanty R, Tuttle M, et al (2002) Denitrification in the recharge area and discharge area of a transient agricultural nitrate plume in a glacial outwash sand aquifer, Minnesota: DENITRIFICATION IN RECHARGE AND DISCHARGE AREAS. *Water Resour Res* 38:10–1–10–26. doi: 10.1029/2001WR000663
- Böhlke JK, Verstraeten IM, Kraemer TF (2007) Effects of surface-water irrigation on sources, fluxes, and residence times of water, nitrate, and uranium in an alluvial aquifer. *Appl Geochem* 22:152–174. doi: 10.1016/j.apgeochem.2006.08.019
- California Stormwater Quality Association (2003), *Stormwater Best Management Practices: Handbook New Development and Redevelopment*, 378 p., Menlo Park, Calif. [Available at <http://www.cabmphandbooks.com/documents/Development/DevelopmentHandbook.pdf>]
- Cao X, Chen Y, Wang X, Deng X (2001) Effects of redox potential and pH value on the release of rare earth elements from soil. *Chemosphere* 44:655–661.
- Clifton HE, Hunter RE, Gardner JV (1988) Analysis of Eustatic, Tectonic, and Sedimentologic Influences on Transgressive and Regressive Cycles in the Upper Cenozoic Merced Formation, San Francisco, California. In: Kleinspehn KL, Paola C (eds) *New Perspect. Basin Anal.* Springer-Verlag, New York, pp 109–128

- Datry T, Malard F, Gibert J (2004) Dynamics of solutes and dissolved oxygen in shallow urban groundwater below a stormwater infiltration basin. *Sci Total Environ* 329:215–229. doi: 10.1016/j.scitotenv.2004.02.022
- Datry T, Malard F, Vitry L, et al (2003) Solute dynamics in the bed sediments of a stormwater infiltration basin. *J Hydrol* 273:217–233. doi: 10.1016/S0022-1694(02)00388-8
- Datry T, Malard F, Gibert J (2006) EFFECTS OF ARTIFICIAL STORMWATER INFILTRATION ON URBAN GROUNDWATER ECOSYSTEMS. *Urban Groundw Manag Sustain* 331–345
- Department of Environmental Resources (1999), Low-Impact Development Hydrologic Analysis, Department of Environmental Resources, Programs and Planning Division, Prince George's County, Maryland. [online] Available from: http://www.lowimpactdevelopment.org/pubs/LID_Hydrology_National_Manual.pdf (Accessed 10 March 2013)
- Dietz ME, Clausen JC (2005) A field evaluation of rain garden flow and pollutant treatment. *Water Air Soil Pollut* 167:123–138.
- Dietz ME, Clausen JC (2006) Saturation to Improve Pollutant Retention in a Rain Garden. *Environ Sci Technol* 40:1335–1340. doi: 10.1021/es051644f
- Elliott A, Trowsdale S (2007) A review of models for low impact urban stormwater drainage. *Environ Model Softw* 22:394–405. doi: 10.1016/j.envsoft.2005.12.005
- Eriksson E, Baun A, Scholes L, et al (2007) Selected stormwater priority pollutants — a European perspective. *Sci Total Environ* 383:41–51. doi: 10.1016/j.scitotenv.2007.05.028
- Fan AM, Steinberg VE (1996) Health implications of nitrate and nitrite in drinking water: an update on methemoglobinemia occurrence and reproductive and developmental toxicity. *Regul Toxicol Pharmacol* 23:35–43.
- Fiedler S, Vepraskas MJ, Richardson JL (2007) Soil redox potential: Importance, field measurements, and observations. *Advances in agronomy*, VOL. 94, pp. 1-54.
- Fischer D, Charles EG, Baehr AL (2003) Effects of stormwater infiltration on quality of groundwater beneath retention and detention basins. *J Environ Eng* 129:464–471.

- Fletcher TD, Andrieu H, Hamel P (2013) Understanding, management and modelling of urban hydrology and its consequences for receiving waters: A state of the art. *Adv Water Resour* 51:261–279. doi: 10.1016/j.advwatres.2012.09.001
- Galloway JN, John D. Aber JD, Erisman JW, Seitzinger SP, Howarth RW, Cowling EB, Cosby BJ (2003). The nitrogen cascade. *BioScience*, Vol. 53, No. 4, pp. 341-356
- Greskowiak J, Prommer H, Massmann G, et al (2005) The impact of variably saturated conditions on hydrogeochemical changes during artificial recharge of groundwater. *Appl Geochem* 20:1409–1426. doi: 10.1016/j.apgeochem.2005.03.002
- Gurdak JJ, Qi SL (2012) Vulnerability of Recently Recharged Groundwater in Principle Aquifers of the United States To Nitrate Contamination. *Environ Sci Technol* 46:6004–6012. doi: 10.1021/es300688b
- Holman-Dodds JK, Bradley AA, Potter KW (2007) EVALUATION OF HYDROLOGIC BENEFITS OF INFILTRATION BASED URBAN STORM WATER MANAGEMENT1. *JAWRA J Am Water Resour Assoc* 39:205–215.
- Joshi UM, Balasubramanian R (2010) Characteristics and environmental mobility of trace elements in urban runoff. *Chemosphere* 80:310–318. doi: 10.1016/j.chemosphere.2010.03.059
- Kenny JF, Barber NL, Hutson SS, et al (2009) Estimated use of water in the United States in 2005. US Geological Survey Reston, VA
- Korom SF (1992), Natural denitrification in the saturated zone: a review. *Water Resour Res*, VOL. 28, NO. 6, pp. 1657-1668.
- Landon MK, Christopher TG, Belitz K, Singleton MJ, Esser BK (2011) Relations of hydrogeologic factors, groundwater reduction-oxidation conditions, and temporal and spatial distributions of nitrate, Central-Eastside San Joaquin Valley, California, USA. *Hydrogeology Journal*, VOL. 19, pp. 1203–1224
- Lu P, Yuan T (2011) Low impact development design for urban stormwater management-A case study in USA. *Water Resour. Environ. Prot. ISWREP 2011 Int. Symp. On*. pp 2741–2744

- Maniquiz MC, Lee S-Y, Kim L-H (2010) Long-Term Monitoring of Infiltration Trench for Nonpoint Source Pollution Control. *Water Air Soil Pollut* 212:13–26. doi: 10.1007/s11270-009-0318-z
- Massmann G, Greskowiak J, Dünnebier U, et al (2006) The impact of variable temperatures on the redox conditions and the behaviour of pharmaceutical residues during artificial recharge. *J Hydrol* 328:141–156. doi: 10.1016/j.jhydrol.2005.12.009
- McMahon PB, Böhlke JK, Christenson SC (2004) Geochemistry, radiocarbon ages, and paleorecharge conditions along a transect in the central High Plains aquifer, southwestern Kansas, USA. *Appl Geochem* 19:1655–1686. doi: 10.1016/j.apgeochem.2004.05.003
- McMahon PB, Böhlke JK, Kauffman LJ, et al (2008) Source and transport controls on the movement of nitrate to public supply wells in selected principal aquifers of the United States: CONTROLS ON THE MOVEMENT OF NITRATE. *Water Resour Res* 44:n/a–n/a. doi: 10.1029/2007WR006252
- McMahon PB, Chapelle FH (2008) Redox Processes and Water Quality of Selected Principal Aquifer Systems. *Ground Water* 46:259–271. doi: 10.1111/j.1745-6584.2007.00385.x
- McMahon PB, Cowdery TK, Chapelle FH, Jurgens BC (2009) Redox Conditions in Selected Principal Aquifers of the United States.
- Newcomer ME, Gurdak JJ, Sklar LS, Nanus L (2014) Urban recharge beneath low impact development and effects of climate variability and change: RECHARGE BENEATH LOW IMPACT DEVELOPMENT AND CLIMATE CHANGE. *Water Resour Res* 50:1716–1734. doi: 10.1002/2013WR014282
- NOAA NCDC (2014), NCDC National Climatic Data Center (NCDC), [online] Available from: <http://www.ncdc.noaa.gov/oa/ncdc.html> (Accessed 31 May 2014)
- Perica S, Dietz S, Heim S, Hiner L, Maitaria K, MartinD, Pavlovic S, Roy I, Trypaluk C, Unruh D, Yan F, Yekta M, Zhao Y, Bonnin G, Brewer D, Chen L, Parzybok T, Yarchoan J (2011) NOAA Atlas 14 Precipitation-frequency Atlas of the United States. [online] Available from: http://www.nws.noaa.gov/oh/hdsc/PF_documents/Atlas14_Volume6.pdf (Accessed 31 July 2014)

- NOAA NWS (2014), NOAA's National Weather Service (NWS), [online] Available from:
http://hdsc.nws.noaa.gov/hdsc/pfds/pfds_map_cont.html?bkmrk=ca#Plots_Section
 (Accessed 05 August 2014)
- Nzewi O, Gilman JA, Bartow G (2010) 2009 Annual Groundwater Monitoring Report, Westside Basin. San Francisco Public Utilities Commission
- Paul MJ, Meyer JL (2001), Streams in the urban landscape: *Annu. Rev. Ecol. Syst.* Vol. 32, pp. 333-365
- Pazwash H (2011) Urban storm water management. CRC Press. p. 81-84
- Pitt R, Field R, Lalor M, Brown M (1995) Urban stormwater toxic pollutants: assessment, sources, and treatability. *Water Environ Res* 260–275.
- PME, Inc (2012), miniDO₂T user's manual, Precision Measurement Engineering, Inc. Available at: <http://www.pme.com/PDFs/Manual.pdf>.
- Ramesh Kumar A, Riyazuddin P (2012) Seasonal variation of redox species and redox potentials in shallow groundwater: A comparison of measured and calculated redox potentials. *J Hydrol* 444-445:187–198. doi: 10.1016/j.jhydrol.2012.04.018
- Rudolf von Rohr M, Hering JG, Kohler H-PE, von Gunten U (2014) Column studies to assess the effects of climate variables on redox processes during riverbank filtration. *Water Res* 61:263–275. doi: 10.1016/j.watres.2014.05.018
- Sansalone JJ, Hird JP, Cartledge FK, Tittlebaum ME (2005) Event-Based Stormwater Quality and Quantity Loadings from Elevated Urban Infrastructure Affected by Transportation. *Water Environ Res* 77:348–365. doi: 10.2175/106143005X51932
- SFPUC (2009) San Francisco stormwater design guidelines. [online] Available at: <http://www.sfwater.org/modules/showdocument.aspx?documentid=2779>
 (Accessed 24 February 2014)
- SFPUC (2010) BMP Fact Sheets. [online] Available at:
<http://www.sfwater.org/modules/showdocument.aspx?documentid=2778>
 (Accessed 12 July 2014)

- Spalding RF, Exner ME (1993), Occurrence of nitrate in groundwater- a review. J. Environ. Qual. VOL.22, pp. 392-402
- Tesoriero AJ, Puckett LJ (2011) O₂ reduction and denitrification rates in shallow aquifers: O₂ REDUCTION AND DENITRIFICATION RATES. Water Resour Res 47:n/a–n/a. doi: 10.1029/2011WR010471
- Thomas CR, Miao S, Sindhoj E (2009) Environmental factors affecting temporal and spatial patterns of soil redox potential in Florida Everglades wetlands. Wetlands 29:1133–1145. doi: 10.1672/08-234.1
- U.S. Environmental Protection Agency (2000) Low impact development (LID) - A literature review.
- US EPA (2009) Incorporating Low Impact Development into municipal stormwater programs. [online] Available at:
<http://www.epa.gov/region1/npdes/stormwater/assets/pdfs/IncorporatingLID.pdf>
 (Accessed 12 July 2014)
- Vaughan KL, Rabenhorst MC, Needelman BA (2009) Saturation and Temperature Effects on the Development of Reducing Conditions in Soils. Soil Sci Soc Am J 73:663. doi: 10.2136/sssaj2007.0346
- Wilson, T.P., 2014, In-situ sediment oxygen demand rates in Hammonton Creek, Hammonton, New Jersey, and Crosswicks Creek, near New Egypt, New Jersey, August–October 2009: U.S. Geological Survey Scientific Investigations Report 2013–5121, 18 p., <http://dx.doi.org/10.3133/sir20135121>.
- Winter TC (1999) Ground water and surface water: a single resource. DIANE Publishing

7.0 Figures and Tables

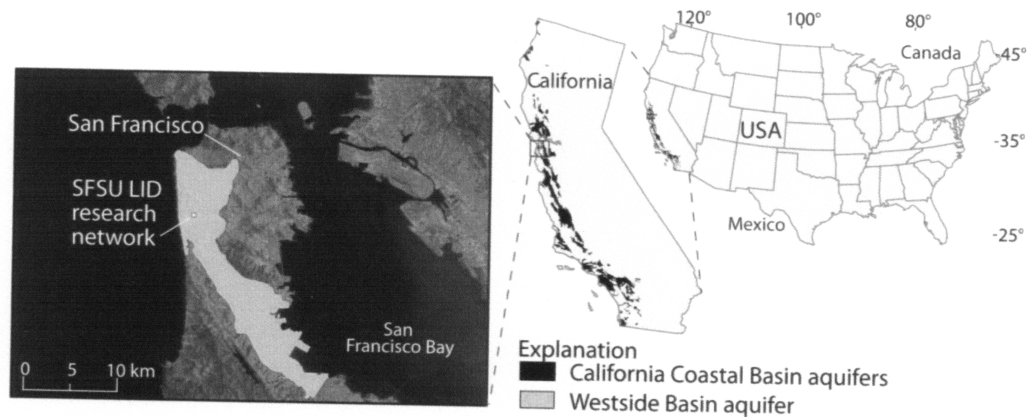


Figure 1. Map showing the location of the San Francisco State University (SFSU) low impact development (LID) research network and the Westside Basin aquifer, which is part of the California Coastal Basin aquifers. The aquifer location data are modified from the California Department of Water Resources and the U.S. Geological Survey. Modified from Newcomer et al., 2014.



Figure 2. Photographs of the infiltration trench at the San Francisco State University (SFSU) low impact development (LID) research network. Modified from Newcomer et al., 2014.

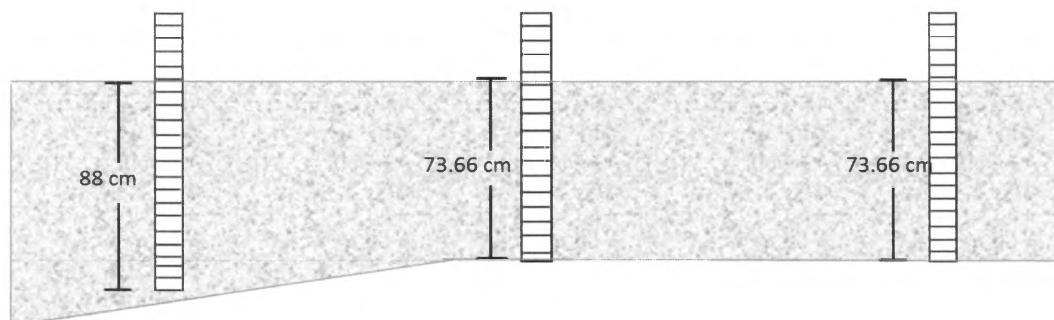


Figure 3. Cross-section of the infiltration trench and the three piezometers with pressure transducers.

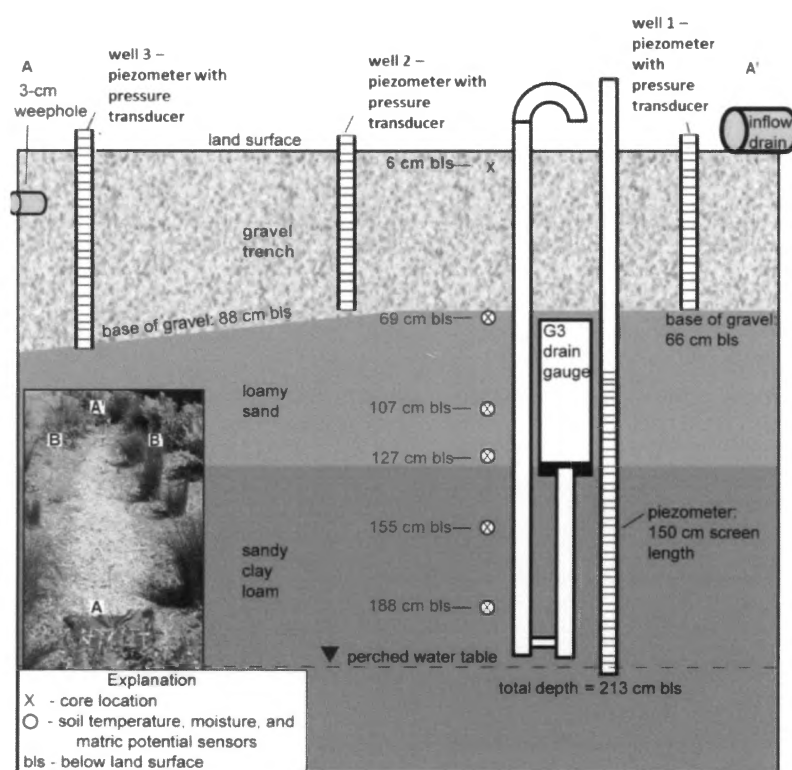


Figure 4. Schematic depiction (not to scale) of the instrumentation and core locations along the longitudinal cross-section A-A' (inset) of the infiltration trench site at the San Francisco State University (SFSU) low impact development (LID) research network. Modified from Newcomer et al., 2014.

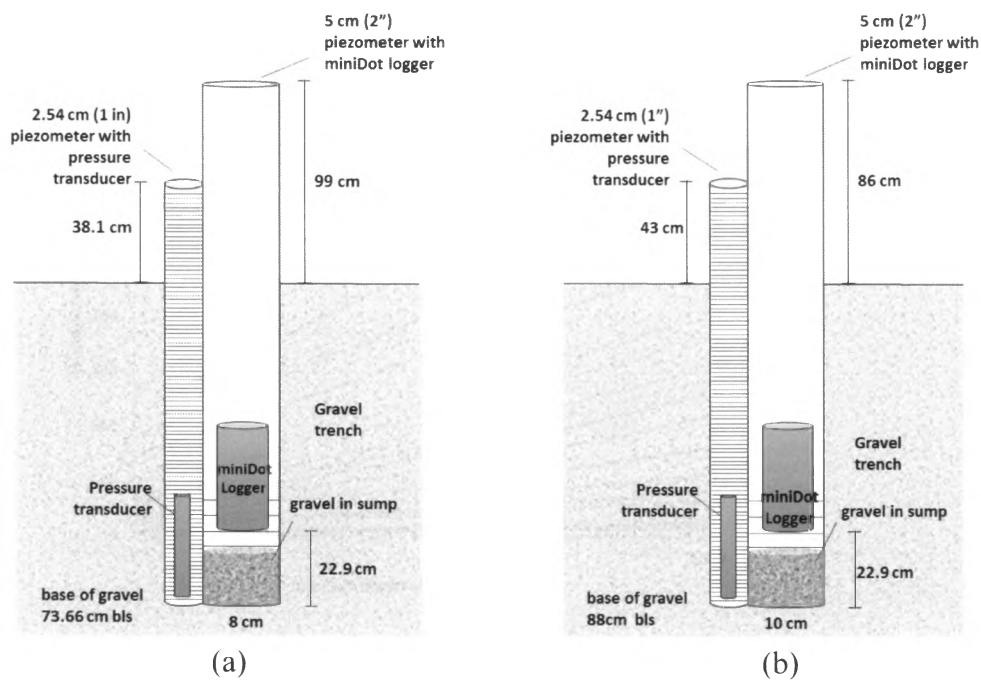


Figure 5. Schematic depiction (not to scale) of the miniDot oxygen loggers and pressure transducers instrumentation and core locations along the infiltration trench site at the San Francisco State University (SFSU) low impact development (LID) research network near (a) Well 1 and (b) Well 3.

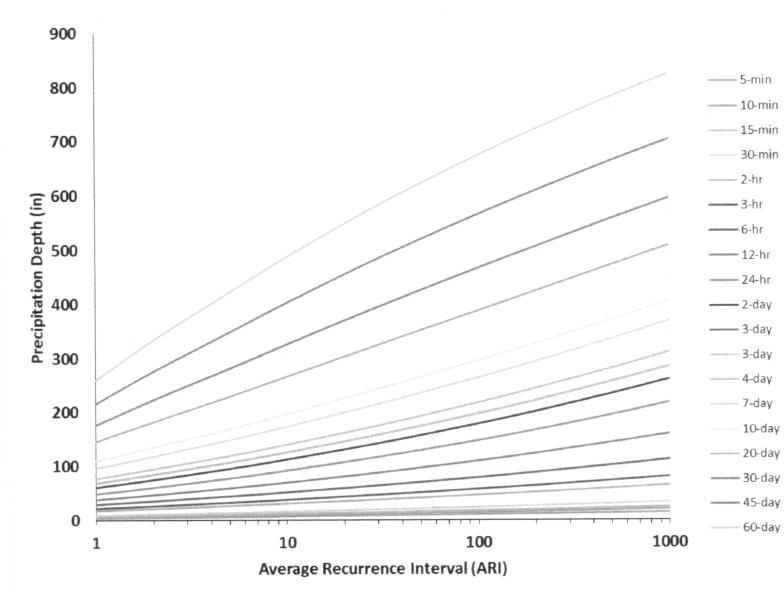


Figure 6. Depth-duration-frequency curve for the San Francisco, Downtown station (NOAA NWS, 2014).

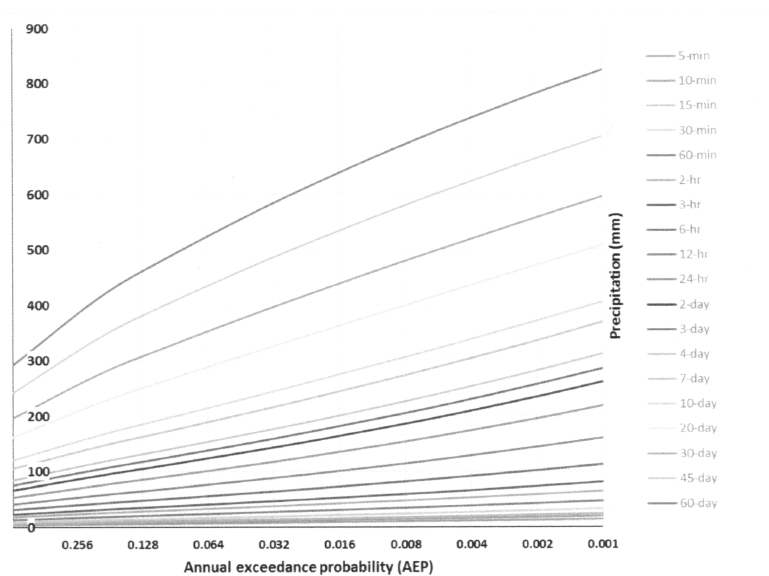


Figure 7. Annual exceedance probability for the San Francisco, Downtown station (NOAA NWS 2014).

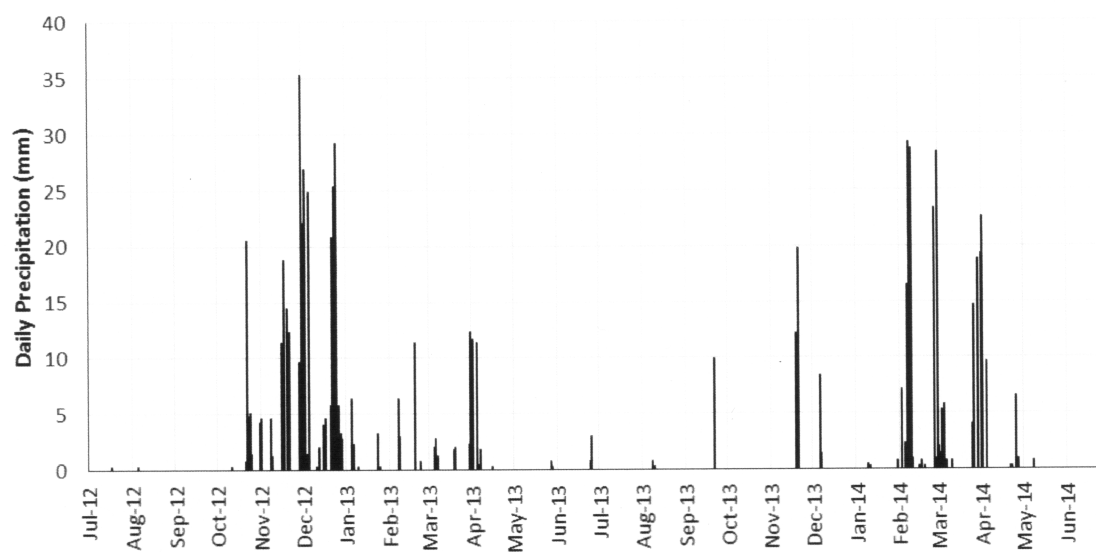


Figure 8. Daily precipitation data from the San Francisco, Downtown station (Station ID: 047772) for the entire data collection period at the LID BMP (July 2012–June 2014) (NOAA NCDC, 2014).

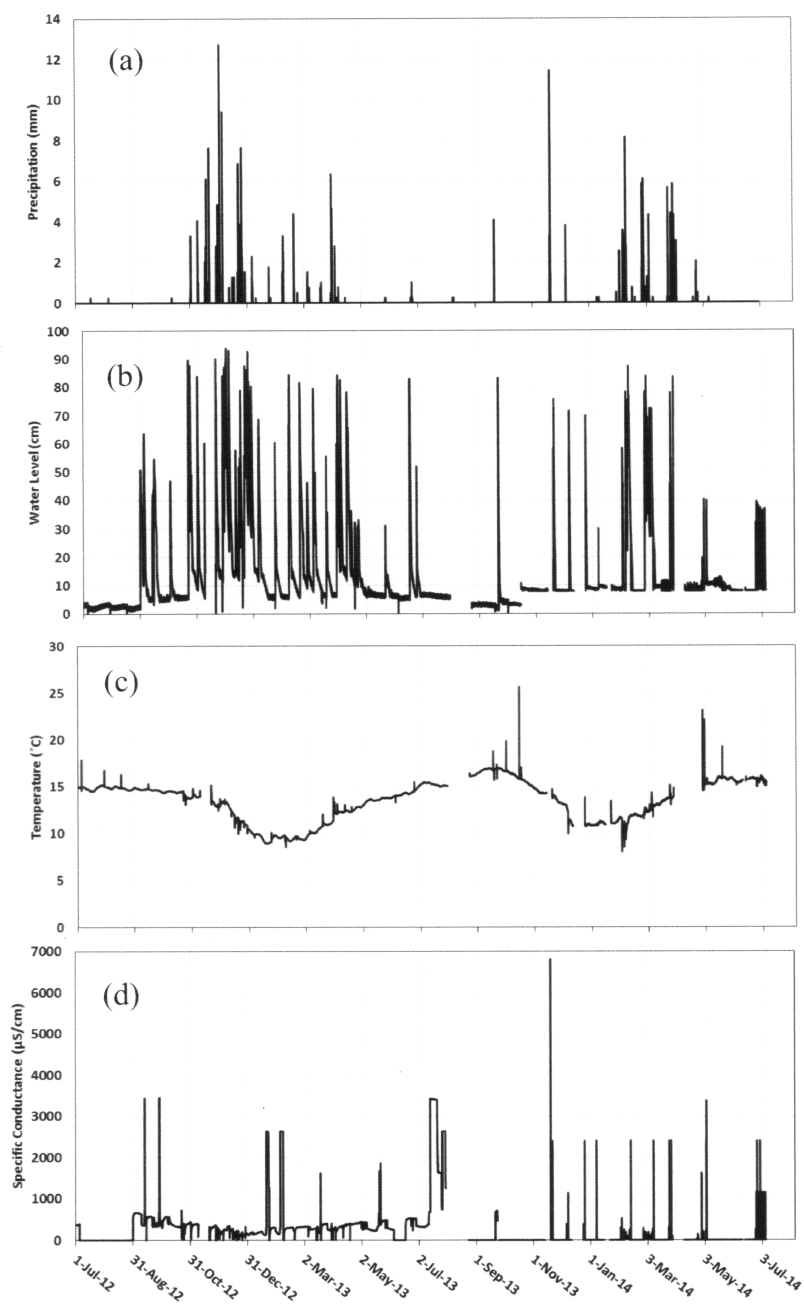


Figure 9. Well#1 (a) hourly timeseries of precipitation. (b) water level in piezometers (c) temperature and (d) Specific Conductance for the period of field observation (July 2012 – June 2014).

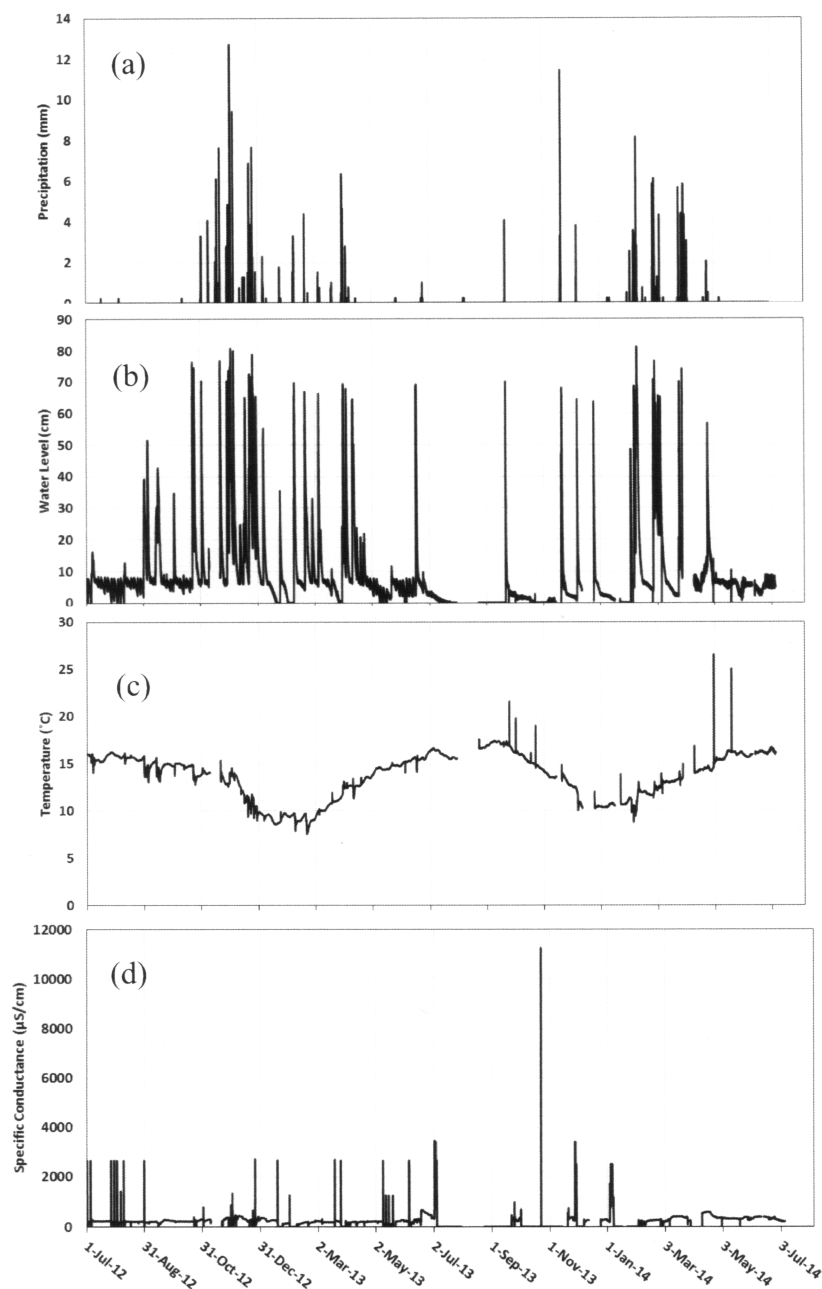


Figure 10. Well#2 (a) hourly timeseries of precipitation. (b) water level in piezometers. (c) temperature and (d) specific conductance for the period of field observation (July 2012 – June 2014).

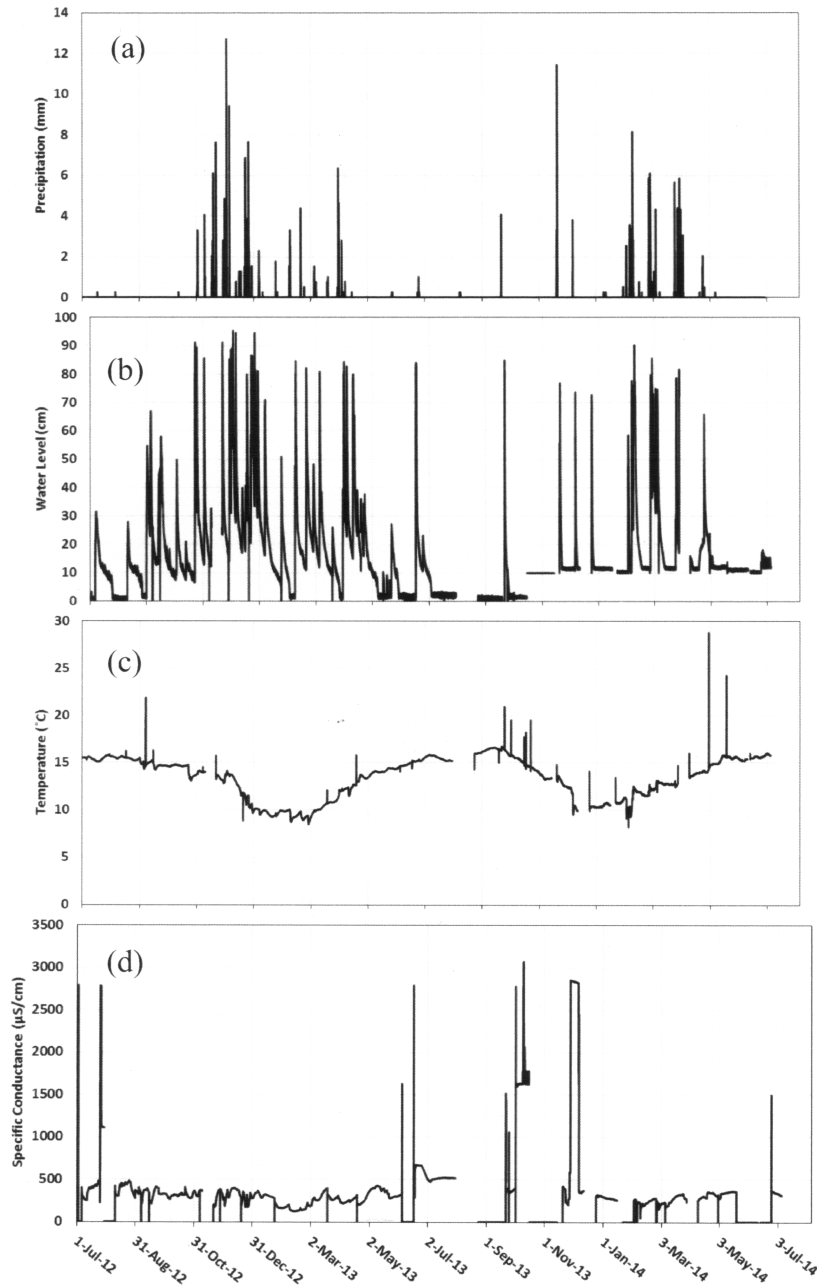


Figure 11. Well#3 (a) hourly timeseries of precipitation. (b) water level in piezometers (c) temperature and (d) specific conductance for the period of field observation (July 2012 – June 2014).

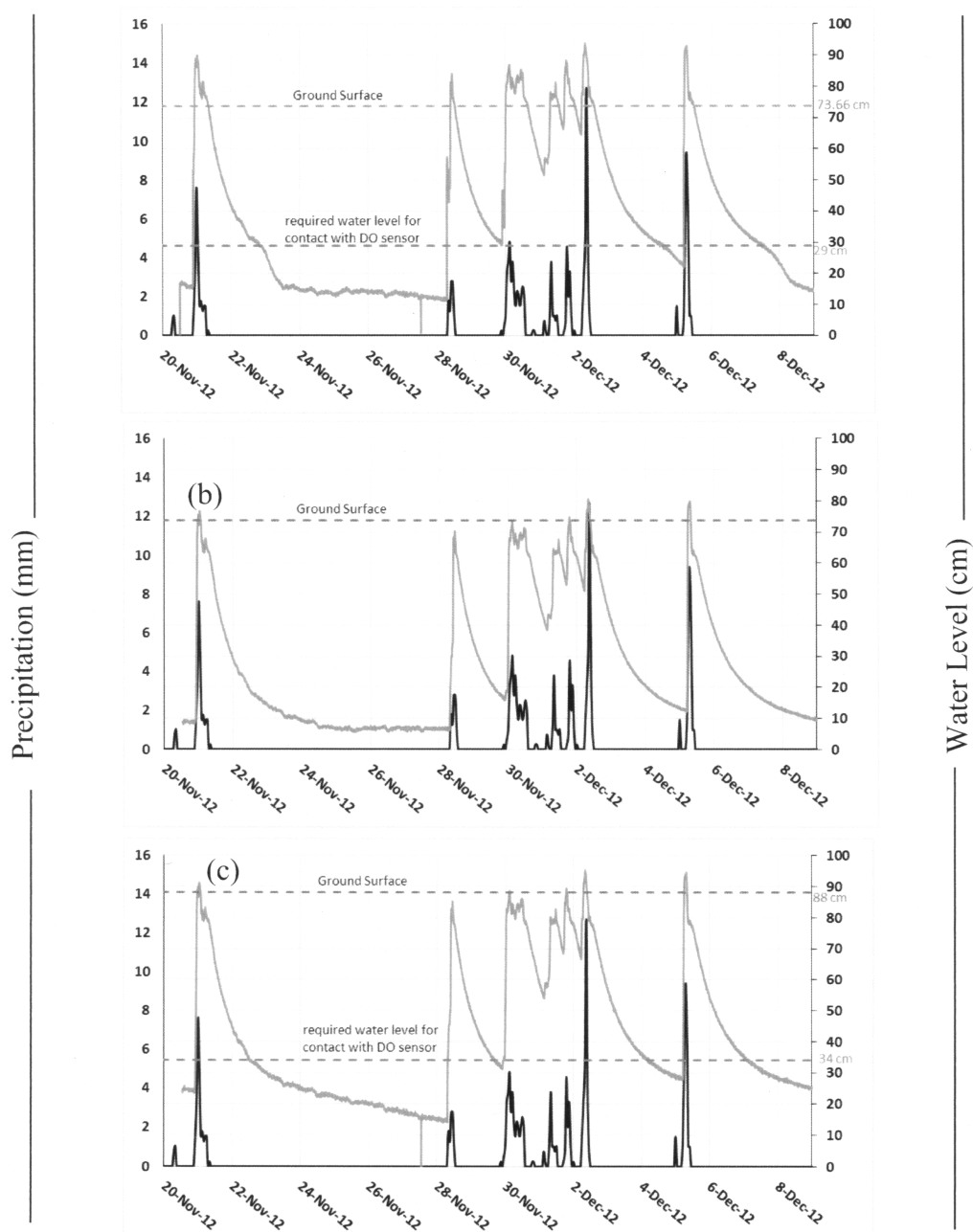


Figure 12. Timeseries of Precipitation (black) and Water levels (blue) in (a) Well 1 (b) Well 2 and (c) Well 3 during rainfall events from November 19, 2012 – December 9, 2012.

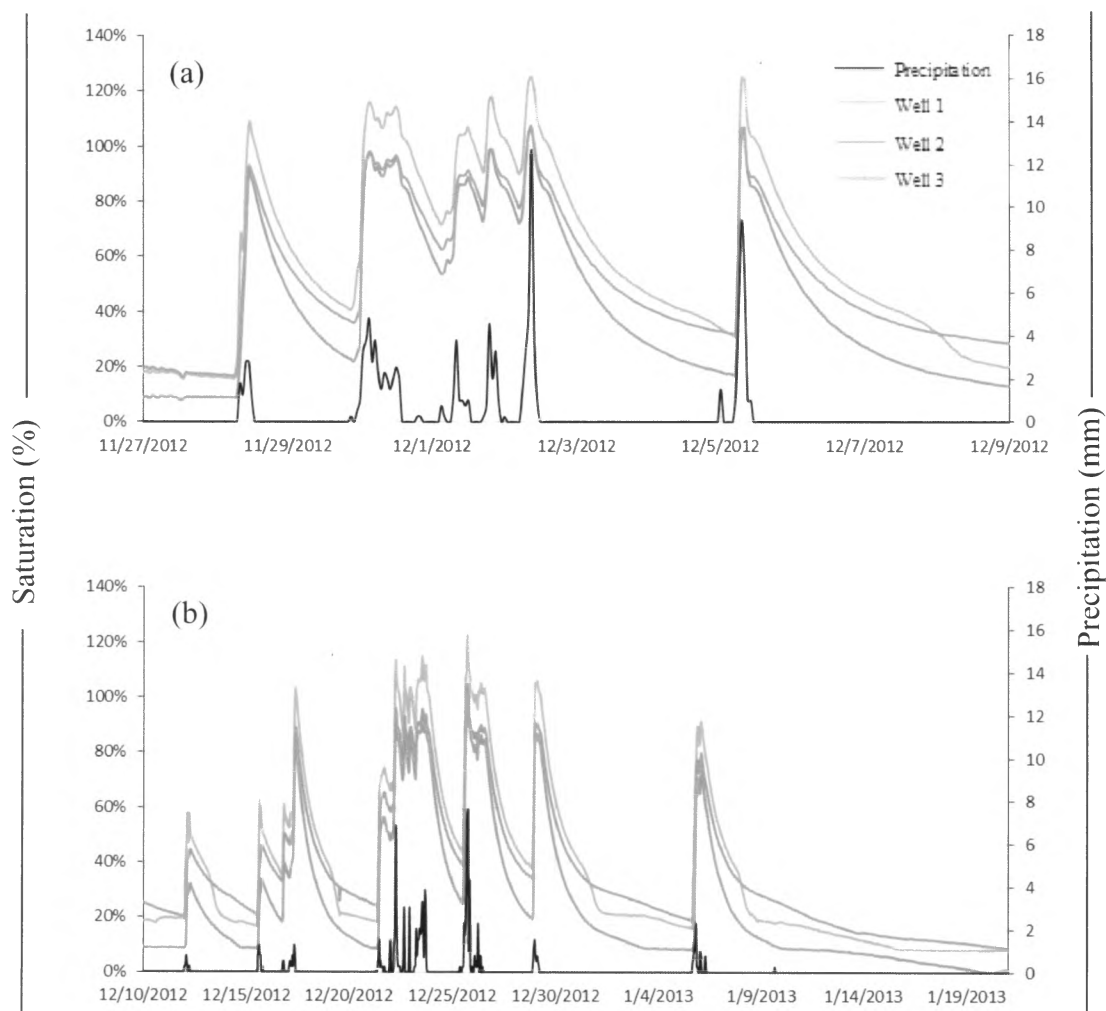


Figure 13. Timeseries of precipitation and % saturation in gravel for all three wells during the rainy season of 2013.

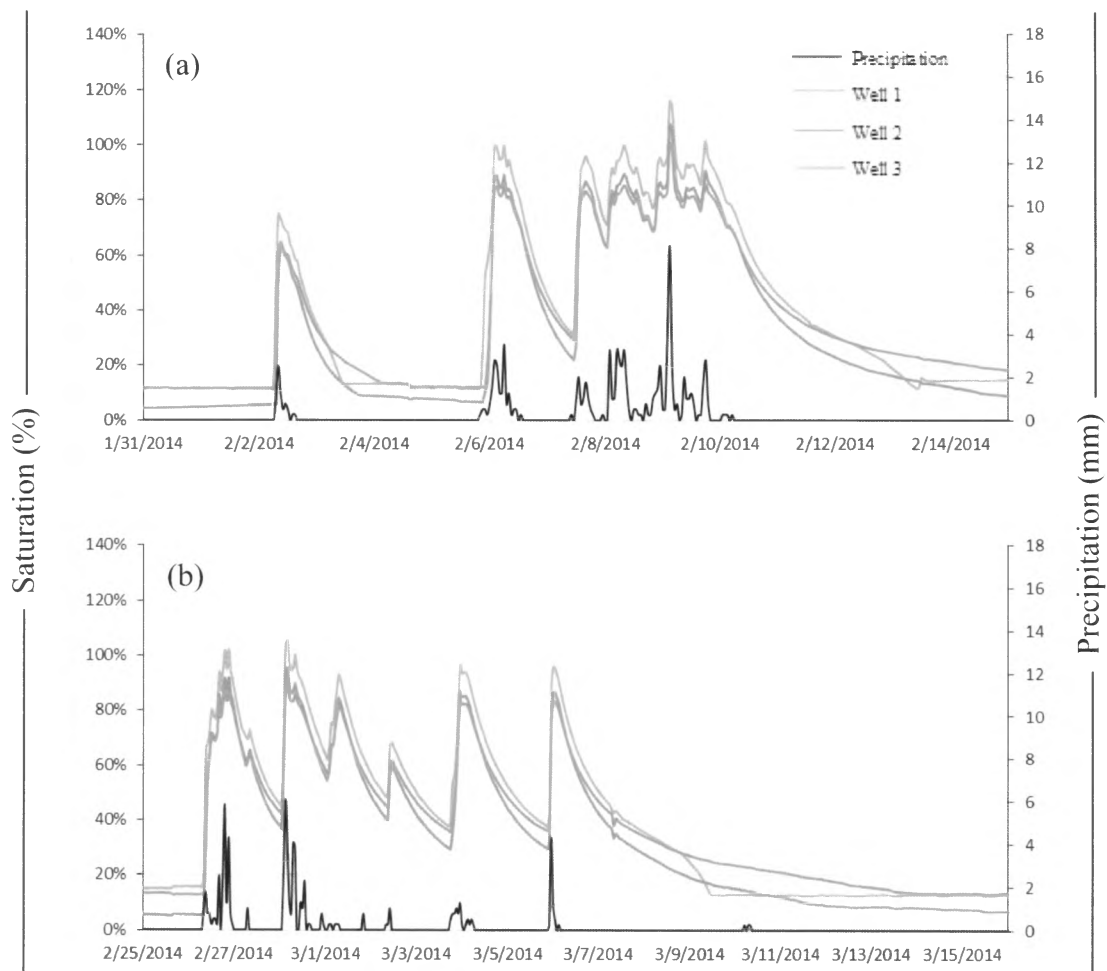


Figure 14. Timeseries of precipitation and % saturation in gravel for all three wells during the rainy season of 2014.

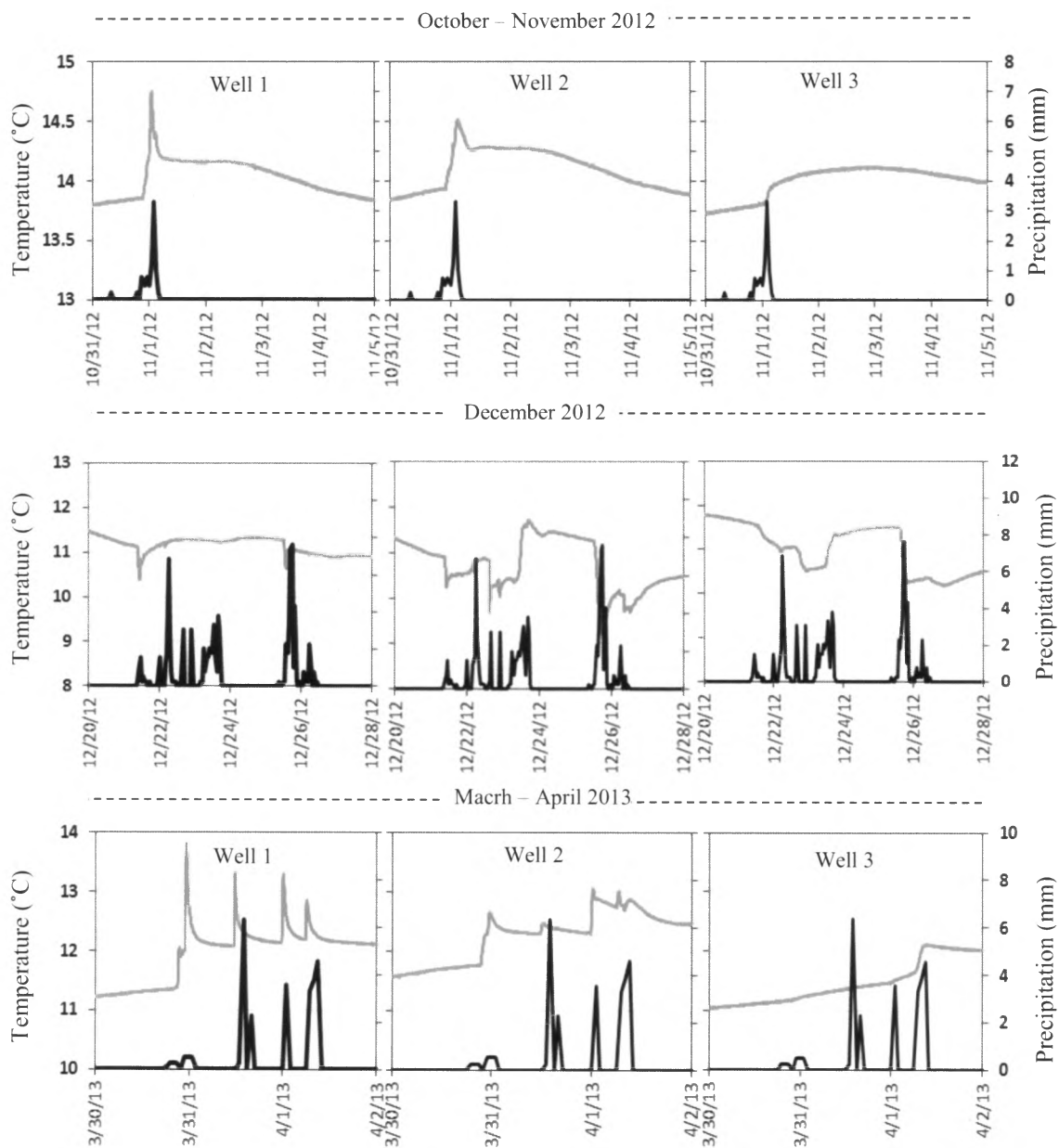


Figure 15. Timeseries for rain events and water temperature occurred on October 31–November 01, 2012, December 20–28, 2012, and March 30 – April 02, 2013 for wells 1, 2, and 3.

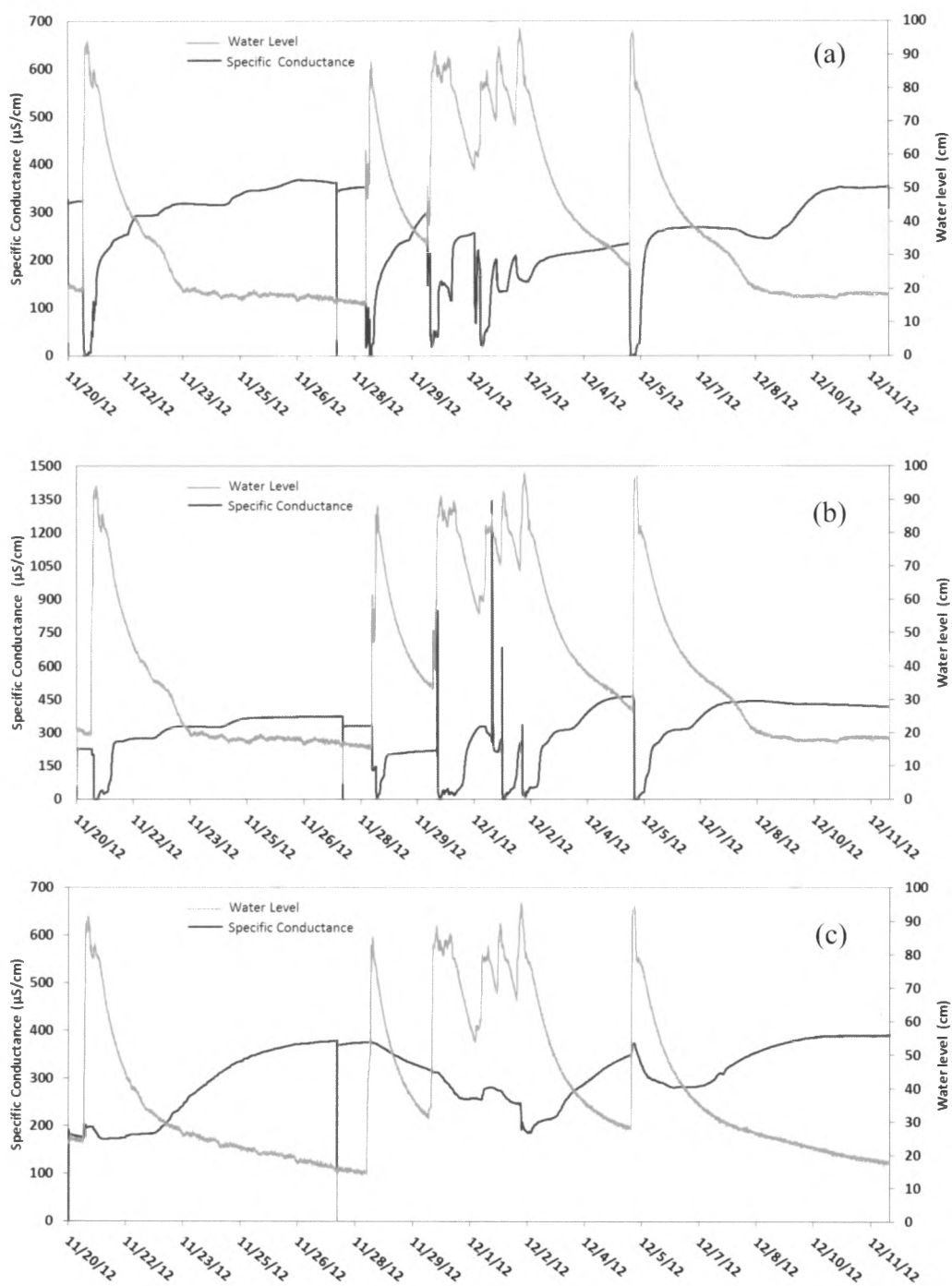


Figure 16. Water levels (blue) and specific conductance (red) for (a) Well 1 (b) Well 2 and (c) Well 3 from November 20 - December 11, 2012.

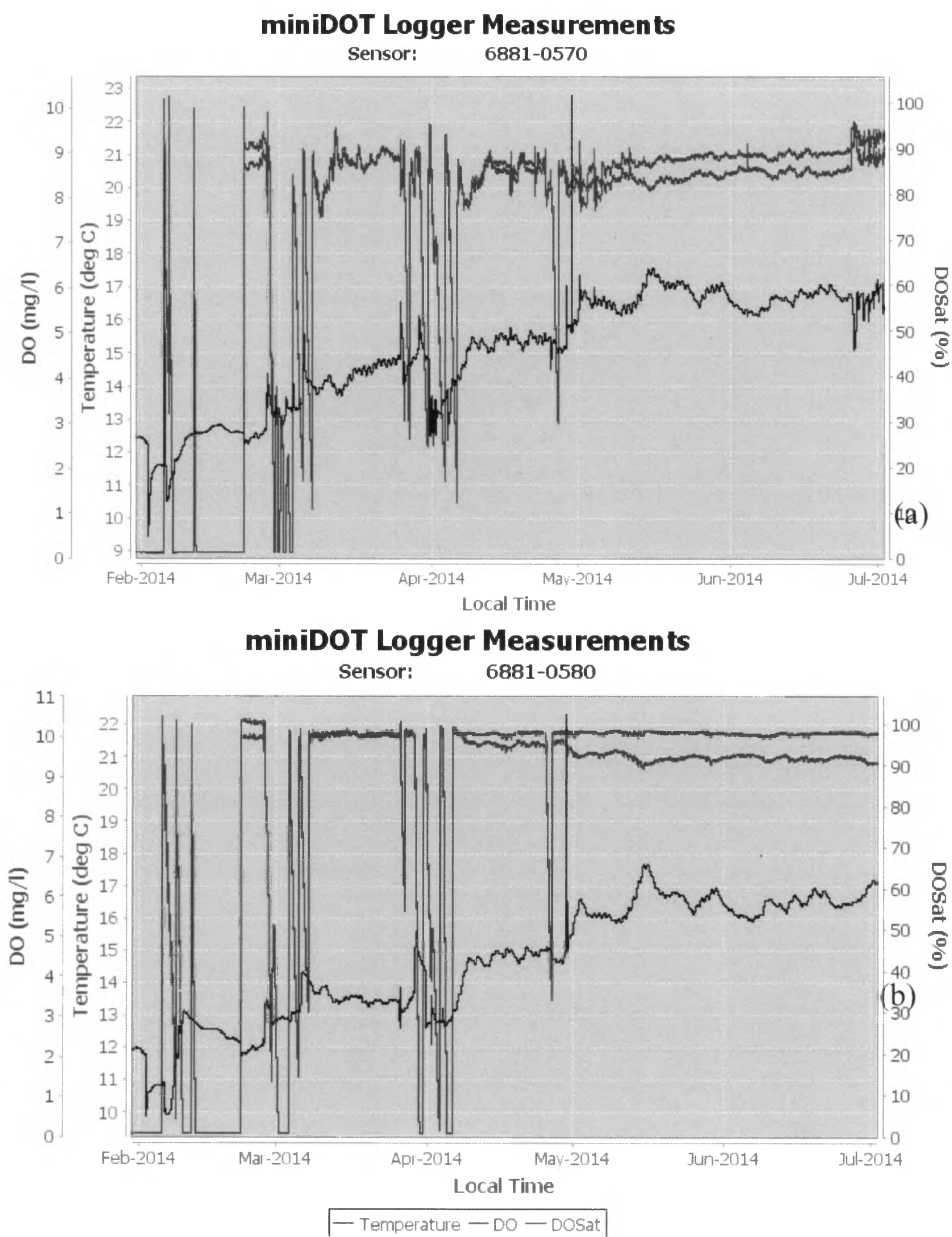


Figure 17. DO concentrations measured continuously by the miniDot loggers in LID trench for the period of field observation February – June 2014 for (a) Well 1 and (b) Well 3.

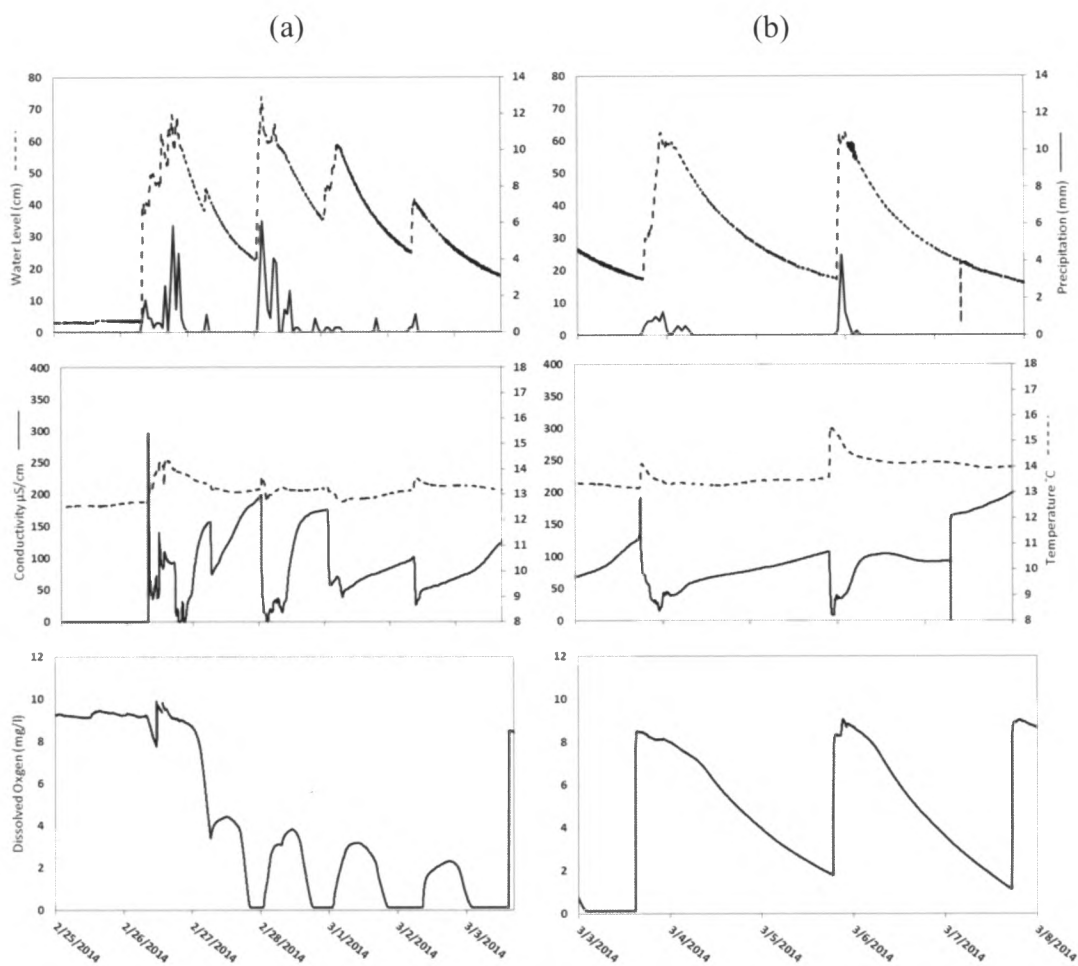


Figure 18. Timesereis of precipitation, water level, temperature, specific conductance, and DO concentration in the LID trench during two rainfall events ((a) February 15 to March 2, 2014, and (b) March 5 to March 8, 2014) of increasing precipitation depth and duration for Well 1.

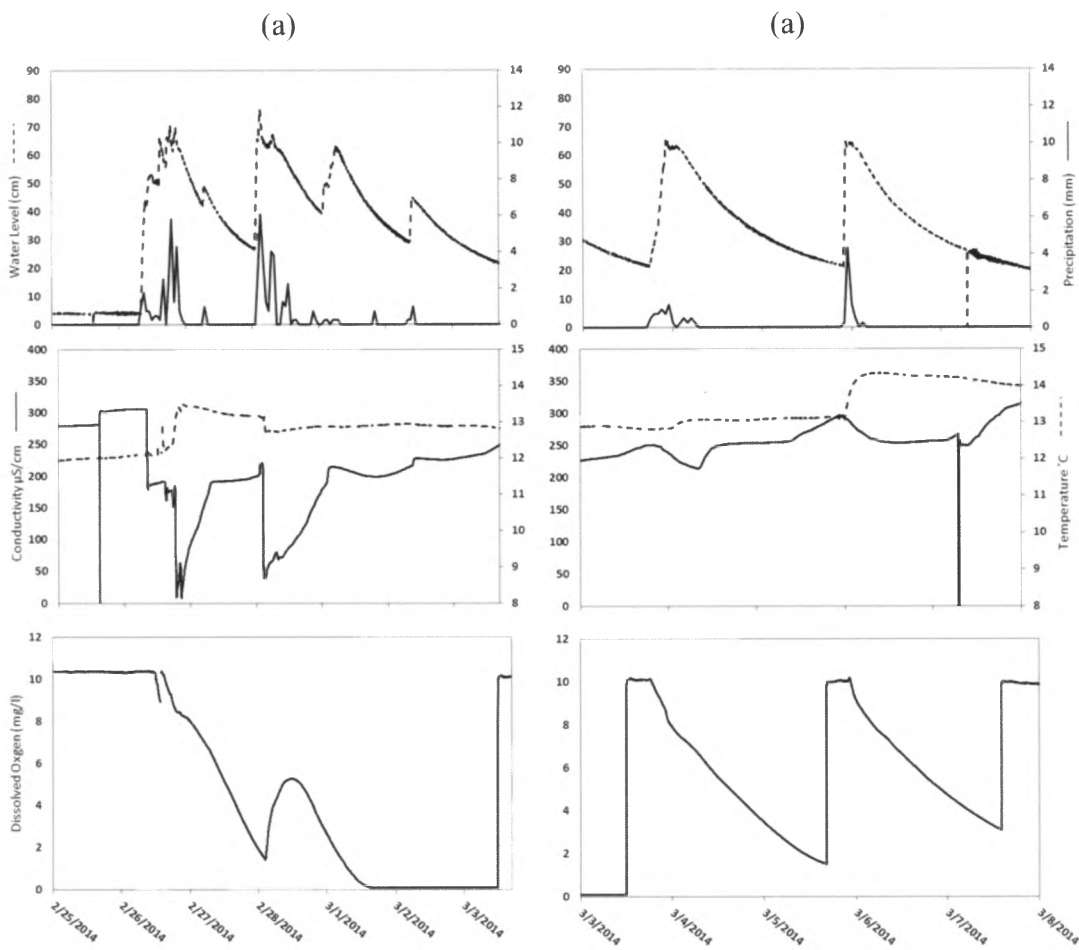


Figure 19. timesereis of precipitation, water level, temperature, specfic conductance, and DO concentration in the LID trench during two rainfall events ((a) February 15 to March 2, 2014, and (b) March 5 to March 8, 2014) of increasing precipitation depth and duration for Well 3.

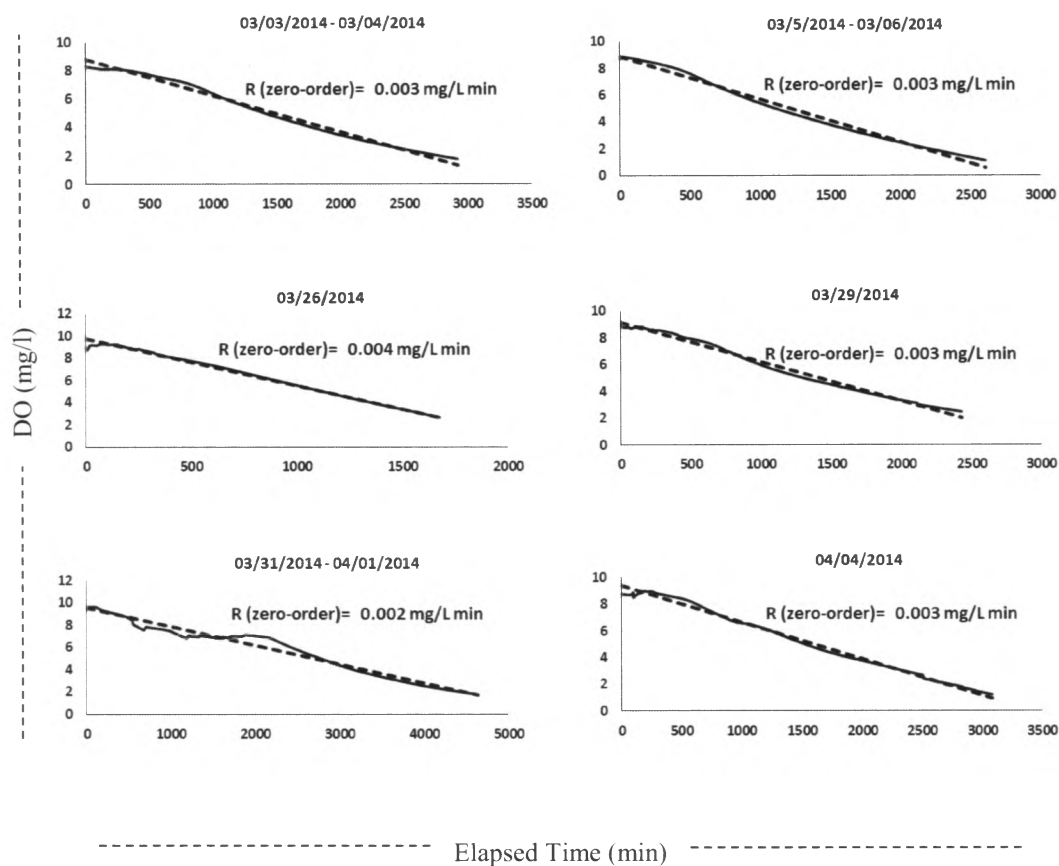


Figure 20. Concentrations of DO in the infiltration trench (during 6 rain events) as a function of elapsed time between beginning of rain event and lowest DO values for that particular rain event, for well 1. Linear regression statistics for the fit of zero-order reaction rate R (mg/L min) are shown for each rain event.

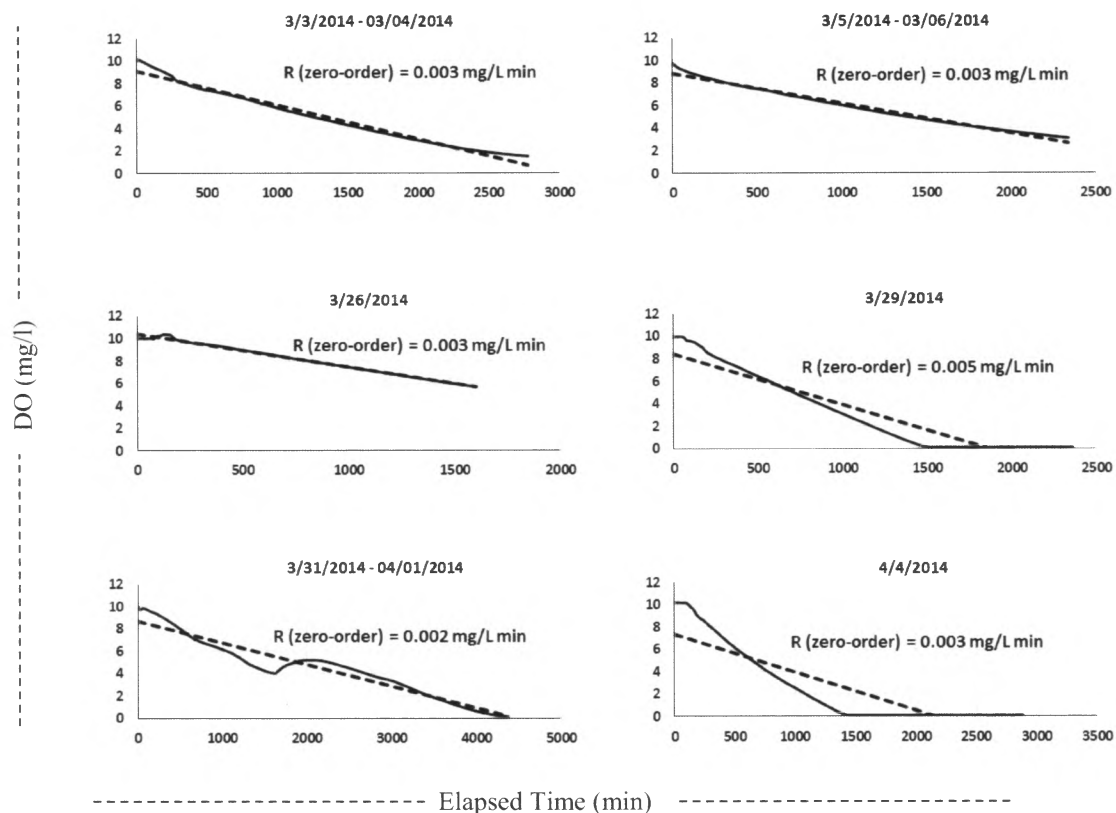


Figure 21. Concentrations of DO in the infiltration trench (during 6 rain events) as a function of elapsed time between beginning of rain event and lowest DO values for that particular rain event, for well 3. Linear regression statistics for the fit of zero-order reaction rate R (mg/L min) are shown for each rain event.

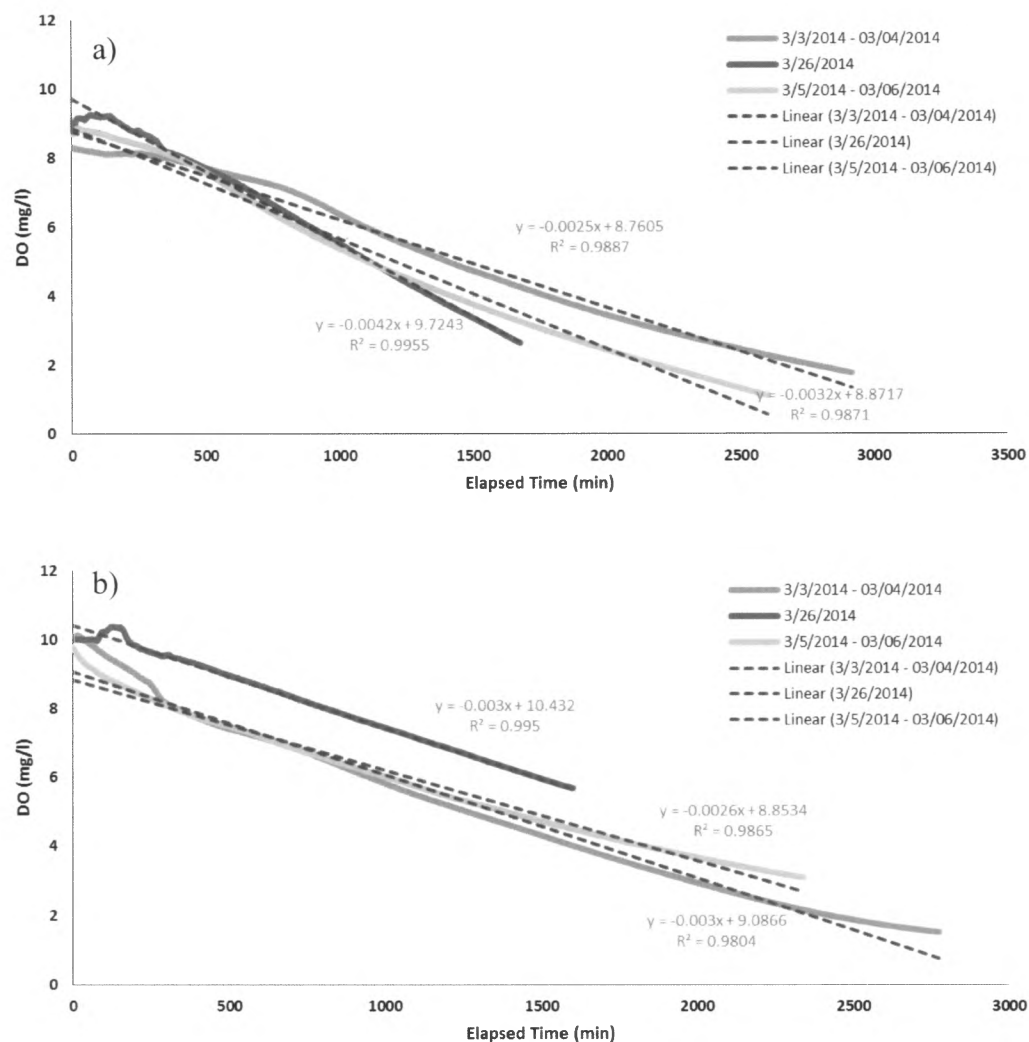


Figure 22. DO depletion curve for a) well 1 and b) well 3 for 3 rain events during the period of field observation (February – June, 2014). The slope of the linear fit for each oxygen-depletion curve [mg/l minute] is used to calculate an average slope of oxygen-depletion curve for the entire infiltration trench.

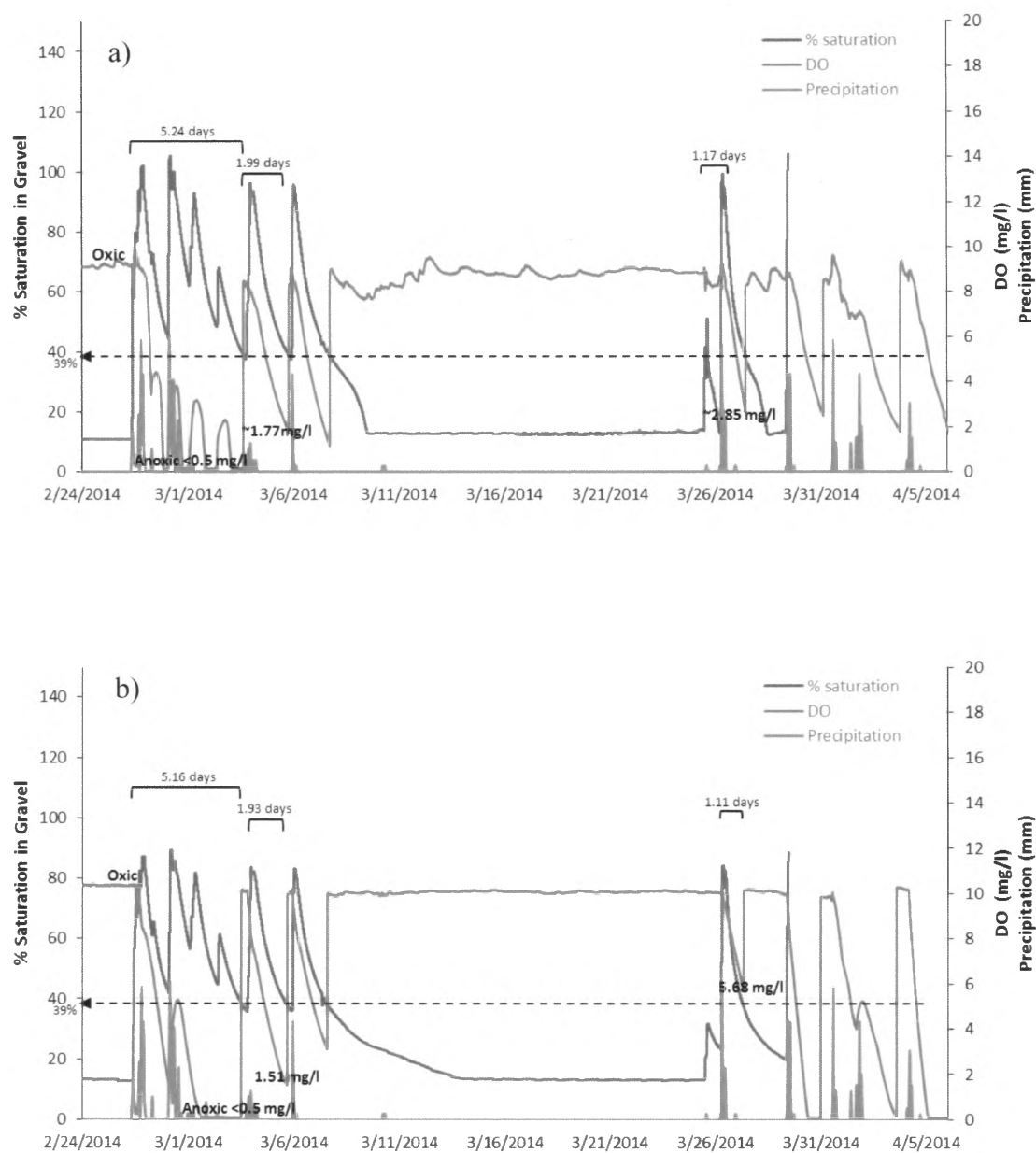


Figure 23. Timeseries of hourly % saturation in gravel (red), DO concentrations (blue), and hourly precipitation (gray) for a) well 1 and b) well 3. % saturation data for the period between March 29 and April 05, 2014 is missing.

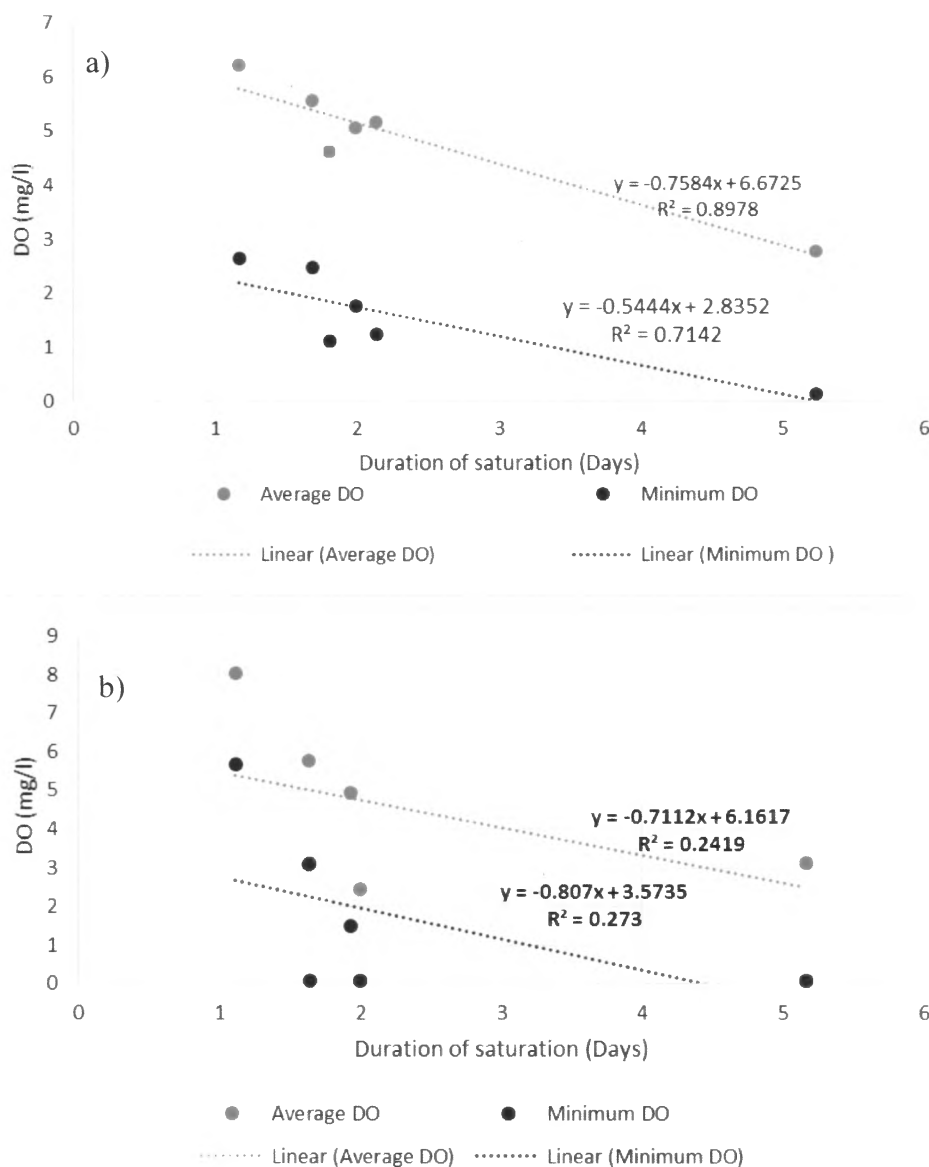


Figure 24. Scatter plot of average and minimum DO vs. duration of saturation for 6 rain events during the period of field observation of DO (February – June 2014) for a) well 1 and b) well 3. General trend shows a negative correlation between the duration of saturation and average and minimum concentrations of DO.

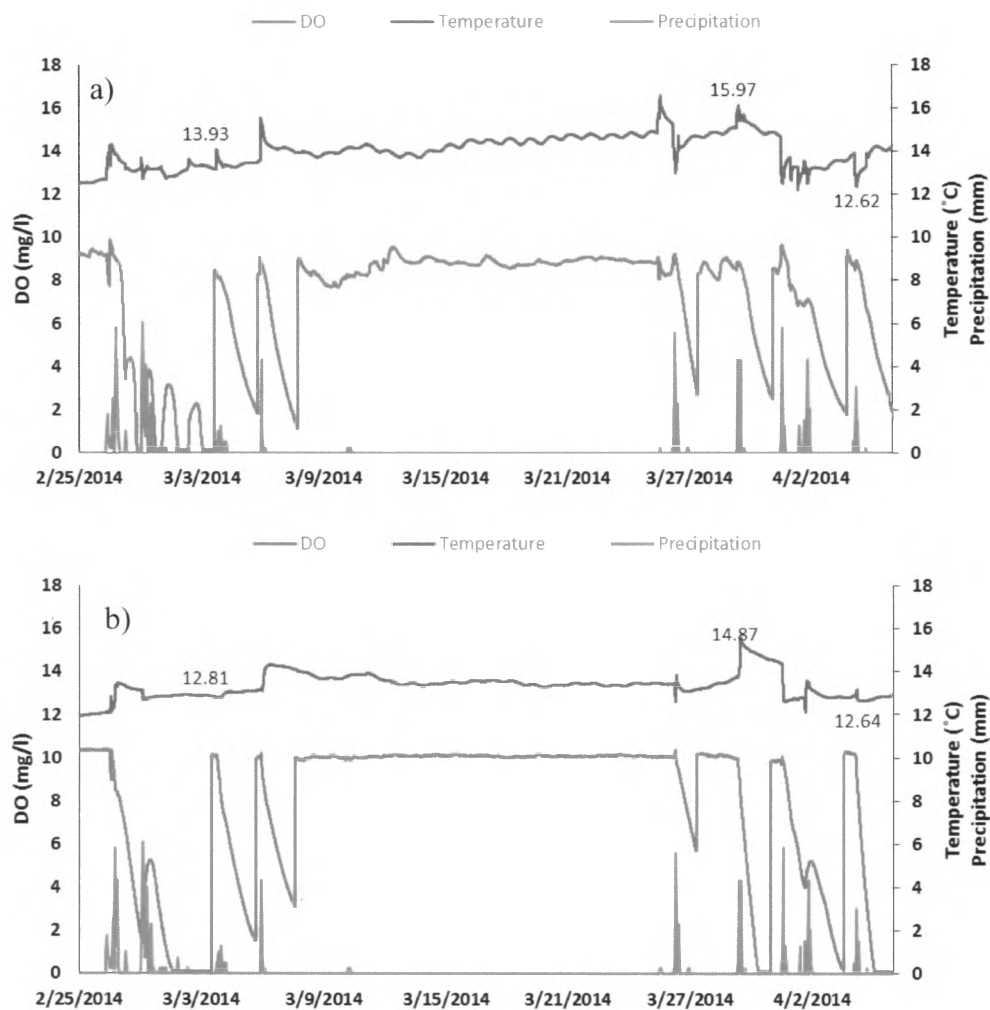


Figure 25. Timeseries of precipitation, DO concentrations, and water temperature for rain events during February – April, 2014, for a) well 1 and b) well3. Numbers above and below temperature series (red) refer to water temperatures under that particular rain event.

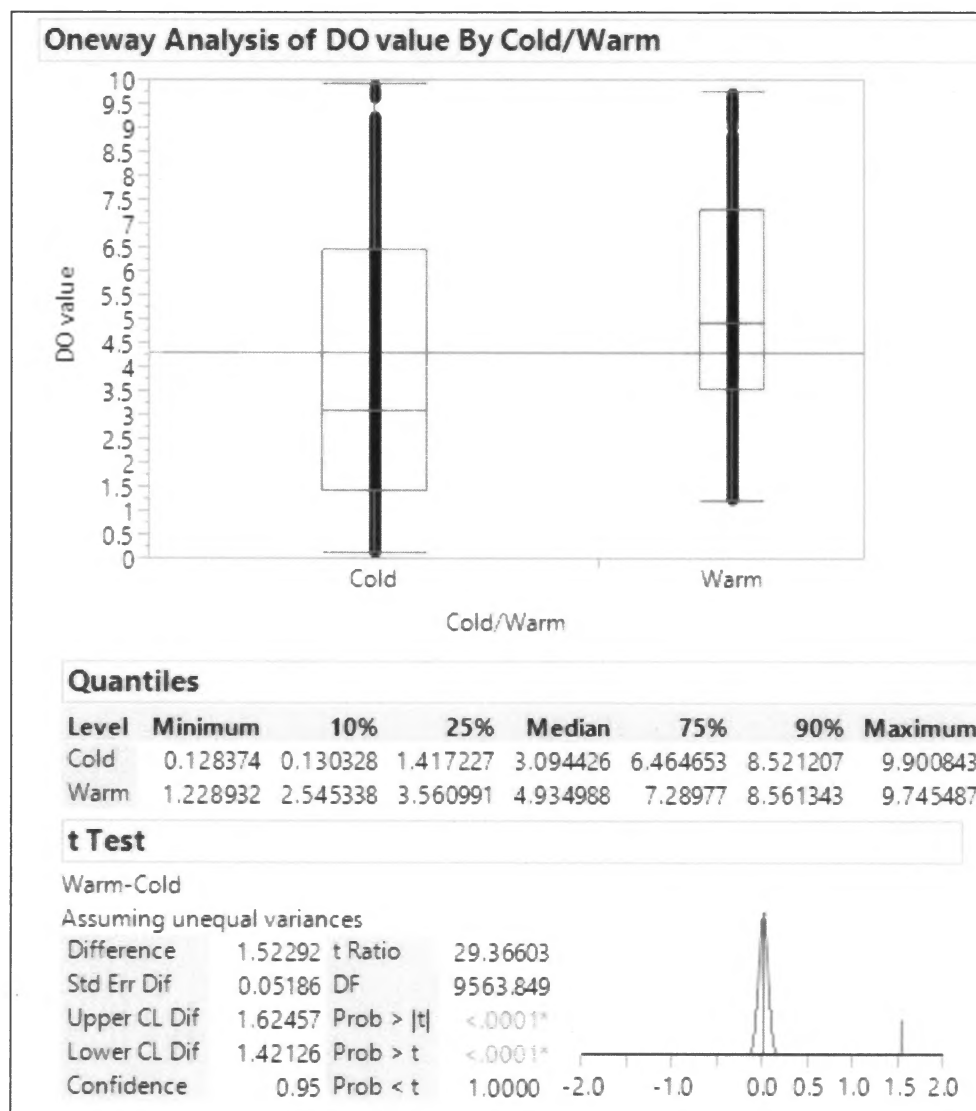


Figure 26. Oneway analysis of DO value for 6 rain events during the period of field observation of DO (February – June, 2014), for well 1.

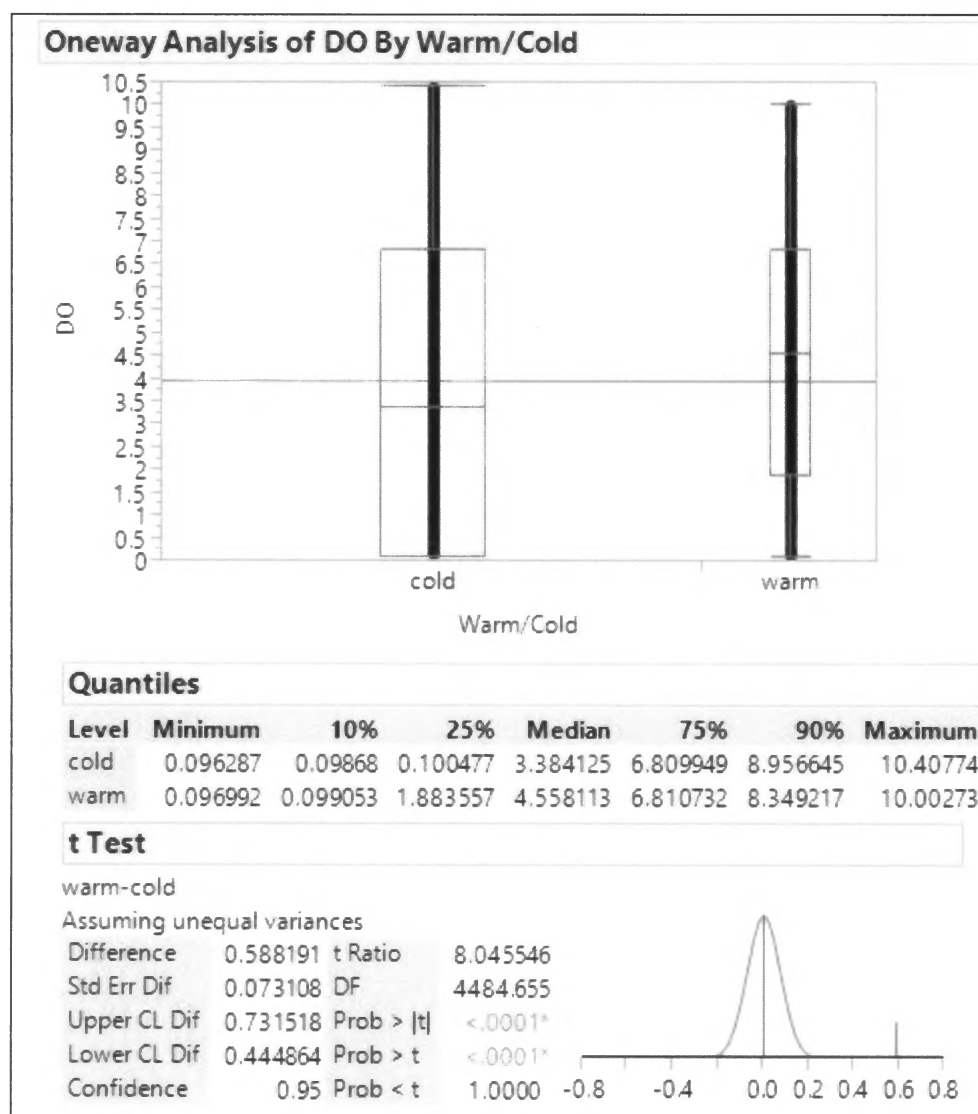


Figure 27. Oneway analysis of DO value for 6 rain events during the period of field observation of DO (February – June, 2014), for well 3.

Table 1. Soil textural and hydraulic properties for cores collected at the infiltration trench. . Modified from Newcomer et al., 2014.

Core Depth (cm bls)	% Sand-Silt-Clay (by vol.)	% Gravel (by mass)	Soil Texture	θ_r ($\text{m}^3 \text{ m}^{-3}$)	θ_s ($\text{m}^3 \text{ m}^{-3}$)	Ks (m d^{-1})
6	0-0-0	1.0×10^2	g	0.00	0.51	8.4×10^2
69	76-8.0-15	87	gsl	0.02	0.15	0.15
107	86-2.0-11	0.3	ls	0.06	0.40	1.7
127	84-4.0-11	0.8	ls	0.05	0.34	0.73
155	64-8.0-27	8.6	scl	0.06	0.32	0.07
188	64-8.0-27	20	scl	0.05	0.29	0.07

Table 2. Precipitation Frequency Estimates for Downtown station, San Francisco (NOAA NWS, 2014).

Recurrence Interval (years)	Precipitation Depth (mm)		
	1- hr	6- hr	24- hr
2	14.99	35.31	60.45
5	18.85	44.20	77.47
10	22.05	51.56	91.95
25	26.42	61.98	112.78
50	29.97	70.36	129.54

Table 3. Zero-order rates of O₂ reduction for wells 1 and 3, for 6 rain event during the period of field observation of DO (February – June, 2014).

Rain-event Date	Total Rainfall Depth (mm)	Well 1		Well 3	
		Zero-Order Rates (mg/L min)	Zero-Order Rates (mg/L hour)	Zero-Order Rates (mg/L min)	Zero-Order Rates (mg/L hour)
Feb 26 – Mar 03, 2014	54.4	0.003	0.15	0.003	0.180
Mar 03 – 04, 2014	5.33	0.003	0.192	0.003	0.156
Mar 05 – 06, 2014	5.84	0.004	0.252	0.003	0.180
Mar 25 – 26, 2014	12.64	0.003	0.174	0.005	0.270
Mar 29, 2014	11.68	0.002	0.102	0.002	0.120
April 04, 2014	6.35	0.003	0.162	0.003	0.204

Table 4. LIDOD_T and LIDOD₂₀ rates in mg/m³ hour for wells 1 and 3, for 3 rain event during the period of field observation of DO (February – June, 2014).

Rain-event Date	Total Rainfall Depth (mm)	Avg. Temperature °C	Well 1		Well 3	
			LIDOD _T mg/m ³ min	LIDOD ₂₀ mg/m ³ min	LIDOD _T mg/m ³ min	LIDOD ₂₀ mg/m ³ min
Mar 03 – 04, 2014	5.33	13.02	1.48	2.23	1.80	2.80
Mar 05 – 06, 2014	5.84	14.17	1.84	2.63	1.52	2.20
Mar 25 – 26, 2014	12.64	13.18	2.49	3.59	1.83	2.81

Table 5. Corresponding durations of saturation and DO concentrations for rain events that occurred between February and April 2014 for well 1.

Rain-event Date	Total Rainfall Depth (mm)	Duration of Saturation (days)	DO mg/L			Avg. Temperature °C
			Avg.	Min	Max	
Feb 26 – Mar 03, 2014	54.4	5.24	2.78	0.13	9.9	13.6
Mar 03 – 04, 2014	5.33	1.99	5.06	1.77	8.22	13.4
Mar 05 – 06, 2014	5.84	1.81	4.71	1.12	8.86	14.27
Mar 25 – 26, 2014	12.64	1.17	6.3	2.85	9.26	14.3
Mar 29, 2014	11.68	1.69	5.57	2.47	8.87	15.17
April 04, 2014	6.35	2.14	5.16	1.23	8.96	13.79

Table 6. Corresponding durations of saturation and DO concentrations for rain events that occurred between February and April 2014 for well 3.

Rain-event Date	Total Rainfall Depth (mm)	Duration of Saturation (days)	DO mg/L			Avg. Temperature °C
			Avg.	Min	Max	
Feb 26 – Mar 03, 2014	54.4	5.16	3.12	0.096	10.41	12.92
Mar 03 – 04, 2014	5.33	1.93	4.92	1.51	10.15	13.02
Mar 05 – 06, 2014	5.84	1.63	5.76	3.09	9.79	14.17
Mar 25 – 26, 2014	12.64	1.11	8.04	5.68	10.39	13.18
Mar 29, 2014	11.68	1.64	3.11	0.097	9.99	14.83
April 04, 2014	6.35	2.00	2.44	0.098	10.20	12.79